ÇUKUROVA UNIVERSITY
INSTITUTE OF NATURAL AND APPLIED SCIENCES

MSc THESIS

Barış ATA

QUADRATIC OPTIMAL CONTROL OF AN INVERTED PENDULUM USING ARTIFICIAL BEE COLONY ALGORITHM

DEPARTMENT OF COMPUTER ENGINEERING

ADANA, 2014

ÇUKUROVA UNIVERSITY
INSTITUTE OF NATURAL AND APPLIED SCIENCES

QUADRATIC OPTIMAL CONTROL OF AN INVERTED PENDULUM USING ARTIFICIAL BEE COLONY ALGORITHM

Barış ATA

MSc THESIS

DEPARTMENT OF COMPUTER ENGINEERING

We certify that the thesis titled above was reviewed and approved for the award of degree of the Master of Science by the board of jury on / /2014

…….	…….	…….
Assoc. Prof. Dr. Ramazan ÇOBAN	Prof. Dr. İlyas EKER	Assoc. Prof. Dr. M. Fatih AKAY
SUPERVISOR	MEMBER	MEMBER

This MSc Thesis is written at the Department of Institute of Natural And Applied Sciences of Çukurova University.
Registration Number:

Prof. Dr. Mustafa GÖK
Director
Institute of Natural and Applied Sciences

ABSTRACT

MSc THESIS

QUADRATIC OPTIMAL CONTROL OF AN INVERTED PENDULUM USING ARTIFICIAL BEE COLONY ALGORITHM

Barış ATA

ÇUKUROVA UNIVERSITY
INSTITUTE OF NATURAL AND APPLIED SCIENCES
DEPARTMENT OF COMPUTER ENGINEERING

Supervisor : Assoc. Prof. Dr. Ramazan ÇOBAN
Year: 2014, Page: 73
Jury : Assoc. Prof. Dr. Ramazan ÇOBAN
: Prof. Dr. İlyas EKER
: Assoc. Prof. Dr. M. Fatih AKAY

This study presents a quadratic optimal controller for an inverted pendulum which is designed with Linear Quadratic Regulator (LQR) using the Artificial Bee Colony (ABC) algorithm.

LQR, an optimal control method, is used for control of the dynamical systems in usual. Main design parameters in LQR are the weighting matrices; however there are no relevant systematic techniques presented to choose these matrices. Generally, selecting weighting matrices is performed by trial and error method since there is no direct relation between weighting matrices and time domain specifications like overshoot percentage, settling time, and steady state error.

In this study LQR is used to control an inverted pendulum system with DC motor as a nonlinear dynamical system and the ABC algorithm which is a swarm intelligence based optimization algorithm is used to select weighting matrices to overcome LQR design difficulties. The simulation results justify that the ABC algorithm is a very efficient way to determine LQR weighting matrices in comparison with a method in literature.

Key Words: Artificial Bee Colony Algorithm, Linear Quadratic Regulator, inverted pendulum.

ÖZ

YÜKSEK LİSANS TEZİ

YAPAY ARI KOLONİSİ ALGORİTMASI İLE BİR TERS SARKACIN KUADRATİK OPTİMAL KONTROLÜ

Barış ATA

ÇUKUROVA ÜNİVERSİTESİ
FEN BİLİMLERİ ENSTİTÜSÜ
BİLGİSAYAR MÜHENDİSLİĞİ ANABİLİM DALI

Danışman : Doç. Dr. Ramazan ÇOBAN
Yıl: 2014, Sayfa: 73
Jüri : Doç. Dr. Ramazan ÇOBAN
: Prof. Dr. İlyas EKER
: Doç. Dr. M. Fatih AKAY

Bu çalışmada, Lineer Kuadratik Regülatör (LQR) ile bir ters sarkacın kontrolü için, Yapay Arı Kolonisi (ABC) optimizasyon algoritmasına dayalı bir metot önerilmiştir.

LQR, genellikle dinamik sistemlerin kontrolünde kullanılan bir optimal kontrol yöntemidir. LQR'ın temel tasarım parametreleri ağırlık matrisleridir ancak bu matrislerin belirlenmesi için önerilmiş sistematik bir metot bulunmamaktadır. Ağırlık matrislerinin değerleri ile yüzde aşımı, yerleşme zamanı ve kararlı hal hatası gibi zaman uzayı performans kriterleri arasında doğrudan bir ilişki olmadığı için bu matrislerin seçimi genellikle deneme yanılma yöntemiyle gerçekleştirilmektedir.

Bu çalışmada DC motorlu bir ters sarkaç için bir LQR kontrolör tasarlanmış ve LQR ağırlık matrislerinin seçiminde sürü zekası temelli bir optimizasyon algoritması olan ABC algoritması kullanılmıştır. Simulasyon sonuçları, ABC algoritmasının literatürde önerilen bir yöntem ile karşılaştırıldığında ağırlık matrislerinin belirlenmesinde daha etkin bir yol olduğunu göstermiştir.

Anahtar Kelimeler: Yapay Arı Kolonisi algoritması, lineer kuadratik regülatör, ters sarkaç.

ACKNOWLEDGEMENTS

The study presented in this thesis was carried out under the supervision of Assoc. Prof. Dr. Ramazan ÇOBAN. I would like to express my sincere gratitude to him for his supervision guidance, patience, motivation, useful suggestions and his valuable time for this work.

I would like to thank members of MSc thesis jury, Prof. Dr. İlyas EKER and Assoc. Prof. Dr. M. Fatih AKAY for their suggestions and corrections.

I would like to thank to Adil Cem ALBAYRAK for his support at the beginning of this study.

I would also like to thank to my family for their support. Finally, thanks to my wife Işıl for her tolerance and patience while I spent many hours for this study. She is always supported and encouraged me, I am very grateful to her all times.

CONTENTS **PAGE**

LIST OF TABLES **PAGE**

LIST OF FIGURES **PAGE**

LIST OF SYMBOLS AND ABBREVIATONS

x	: Cart position
θ	: Pendulum angle
M	: Cart mass
m	: Pendulum mass
l	: Pendulum length
g	: The acceleration due to gravity
F	: The force applied to cart
b	: The cart friction coefficient
J_p	: Pendulum moment of inertia
d	: Pendulum damping coefficient
N	: The horizontal component of the reaction force
P	: The vertical component of the reaction force
x_G	: Horizontal coordinate of the center of gravity
y_G	: Vertical coordinate of the center of gravity
τ	: Torque
R	: Rotor circuit resistance
L	: Rotor circuit inductance
T_m	: Rotor Torque
θ_m	: Rotor speed
i	: Armature current
e	: The applied armature voltage
B	: Magnetic field flux density
l_c	: Length of the conductance
K_b	: Back electromotive force
V_b	: Input voltage
ω	: Rotor angular velocity
K_t	: Torque constant

J_m : Rotor moment of inertia

D : Viscous damping

ρ : Pulley radius

n_1 : Gear ratio

K_g : Tuning gain

n_2 : Gear ratio

u : The control signal

y : The output signal

K : Feedback gain matrix

J : Quadratic performance index

SN : Number of solutions

x_i : Solution

D_{op} : Number of the optimization parameters

MCN : Maximum cycle number

p_i : Probability value

fit_i : Fitness value of the solution

Φ_{ij} : Random number

f_{sum} : Objective function

t_s : Settling time

os : Overshoot

e_{ss} : Steady-state error

ψ : Penalty coefficient

$\bar{N}$: Pre-compensation scale factor

r : Reference signal

h : Step size

ABC : Artificial Bee Colony

DC : Direct current

DE : Differential Evolution

GA	: Genetic Algorithm
IFAC	: International Federation of Automatic Control
LQR	: Linear Quadratic Regulator
LTI	: Linear Time-Invariant
PSO	: Particle Swarm Optimization

1. INTRODUCTION

Optimal control has taken up more space in industry and electrical home appliances day by day since its birth in 1697, especially, after the Industrial Evolution controlling of the technical processes became an important field of study. With the start of Automation some easy controlling tasks began to transfer to technical expedient resources which were usually electrical circuits. In these days, processes are controlled by electronic devices and computers at much higher levels and automatic control is becoming a part of daily life. With help of the digital computers regardless of hardware constraints on electrical and electronic circuit elements nowadays many control tasks are carried out by encoding the relevant control algorithms in computer programs. Developments on automatic control still go on and one of the standard tools in control laboratories has been inverted pendulum since 1950's (Astrom and Futura, 2000).

The control of inverted pendulum is a classic example for design, testing, and comparing of different control techniques as a consequence the control of inverted pendulum has been a research interest in the field of control engineering and it has been determined as a benchmark control problem by the International Federation of Automatic Control (IFAC Theory Committee, 1990).

Inverted pendulum is a challenging control problem due to the various characters of system: highly unstable, nonlinear, non-minimum phase and under-actuated mechanical system. Also a reason behind the extensive studies of the inverted pendulum is that several important control systems can be modelled with the help of inverted pendulum (Anderson 1989). Inverted pendulum reveals many interesting system-theoretic properties and its dynamics are fundamental to maintenance balance, such as walking and two-wheeled robots (Kuo, 2007; Jeong and Takahash, 2007).

The inverted pendulum system set up consists of a cart, a pendulum, a DC motor and a driving mechanism. In this system, an inverted pendulum is attached to a cart equipped with a DC motor that drives it along a horizontal track. The inverted pendulum system has two equilibria; stable and unstable. The stable equilibrium is a

state in which pendulum is pointing downwards and the absence of any control force the system turns this state naturally. The second one is unstable equilibrium in which the pendulum is pointing upwards and requires a control force to maintain this state. Hence, there are two control objectives for inverted pendulum system. First one is swing the pendulum up to unstable equilibrium from stable equilibrium and the second one is to maintain the unstable equilibrium position. This study will focus on design of an optimal controller for the second control objective for inverted pendulum system. During this study Feedback Instruments' digital pendulum system is used as a model to create a more realistic control system (Feedback Instruments, 2006).

Optimal control theory is a mathematical optimization method as an extension of the calculus variation and it has numerous applications in control engineering. The main objectives of optimal control theory are determination of the control signals that will cause a process to meet the physical constraints and also maximization or minimization of some performance criteria (Kirk, 1970). A special case of the general optimal control problem where the cost function is a quadratic function and the system dynamics are described by a set of linear differential equations is a linear quadratic optimal control problem. Linear quadratic optimal control is very important for modern control theory by reason of it can be implemented in numerous control engineering problems and also it provides a basis for many other control techniques (Athans, 1966; Kirk, 1970). One of the main solutions for linear quadratic optimal control problem is Linear Quadratic Regulator (LQR). LQR has a simple process that can achieve the closed loop linear quadratic optimal control with linear state or output feedback (Kalman, 1964; Kwakernaak and Sivan, 1972).

Main design parameters of LQR are the weighting matrices; however selection of suitable weighting matrices to shape control input is the most difficult part of LQR (Da Fonseca Neto et. al, 2010). Generally selecting of these matrices is performed by trial and error method which is based on designer's experience and time consuming. Various methods have been suggested to select suitable weighting matrices (Kalman, 1964; Yaoqing, 1992). However there are no relevant systematic

techniques for selecting weighting matrices to satisfy time domain specifications such as overshoot percentage, settling time, and steady state error.

One of the methods for choosing weighting matrices for linear quadratic control is Bryson's rules (Bryson and Ho, 1975). According to this method Q can be taken as $Q = C^T \bar{Q} C$. Since C matrix includes important outputs, these states can enter the cost. $\bar{Q}$ and R are chosen as diagonal matrices so a fixed percentage of change of each variable makes an equal contribution on the cost. For example, supposing a system with single input and four outputs with maximum deviations $u_{\max}, m_1, m_2, \mathrm{m}_3,$ and m_4. The cost for $\bar{Q}$ is $\bar{q}_{11} y_1^2 + \bar{q}_{22} y_2^2 + \bar{q}_{33} y_3^2 + \bar{q}_{44} y_4^2$. According the Bryson's rules if $y_1 = \alpha m_1, y_2 = \alpha m_2, y_3 = \alpha m_3$, and $y_4 = \alpha m_4$, then $\bar{q}_{11} y_1^2 = \bar{q}_{22} y_2^2 = \bar{q}_{33} y_3^2 = \bar{q}_{44} y_4^2$; thus $\bar{q}_{11} \alpha^2 m^2{}_1 = \bar{q}_{22} \alpha^2 m^2{}_2 = \bar{q}_{33} \alpha^2 m^2{}_3 = \bar{q}_{44} \alpha^2 m^2{}_4$. A satisfactory solution for elements of $\bar{Q}$ matrix is then $\bar{q}_{11} = 1/m_1^2$, $\bar{q}_{22} = 1/m_2^2$, $\bar{q}_{33} = 1/m_3^2$, and $\bar{q}_{44} = 1/m_4^2$. Similarly, for R can be defined as $r_{11} = 1/u_{\max}^2$ (Bryson and Ho, 1975).

Also another method for choosing weighting matrices for linear quadratic control of an inverted pendulum is proposed by Ghosh et al. in 2012. According to this method, the Q matrix can be chosen as $Q = diag\{q_{11}\ q_{22}\ q_{33}\ q_{44}\}$ where q_{11} is the weight on cart position, q_{22} is the weight on cart velocity, q_{33} is the weight on pendulum angle, and q_{44} is the weight on pendulum angular velocity. Also R matrix can be chosen as $R = r_{11}$ where r_{11} as a scalar, since the system has a single input. Cart position has the most difficult constraint on pendulum system, hence it is chosen as $q_{11} \gg q_{22}, q_{33}, q_{44}$. In a pendulum system position of the cart must change immediately to prevent the pendulum from falling when the pendulum starts to fall from upright position, thus weight on cart velocity must be higher than weight on pendulum angular velocity, $q_{22} \gg q_{44}$. Since the pendulum angle must be kept in upright position to satisfy constraints, it can be chosen as $q_{33} \gg q_{44}$. Overall the weight can be chosen as $q_{11} \gg q_{22}, q_{33} \gg q_{44}$. Also constraint on control signal magnitude can be chosen as $r_{11} \gg 1$. To satisfy these constraints the weights can be

determined as $q_{11} = 500q$, $q_{22}, q_{33} = 20q$, $q_{44} = q$, and $r_{11} = 10^n$ where q and n should be found out(Ghosh et al., 2012).

Beside these methods, recently many researchers have proposed artificial intelligence algorithms such as Genetic Algorithms (GA) (Bottura and Da Fonseca Neto, 2000) and Particle Swarm Optimization (PSO) algorithm for this goal (Mobayen et. al, 2011). Another swarm intelligence based algorithm the Artificial Bee Colony (ABC) algorithm can also be used for selecting weighting matrices.

The ABC algorithm was introduced by Karaboga in 2005 as a new method in the field of swarm intelligence. The ABC is based on the intelligent behavior of honey bee swarms finding nectar as food and sharing the information of these food resources with each other to optimize numeric benchmark function optimization problems (Karaboga, 2005). Then it was extended by Karaboga and Basturk and presented to transcend other recognized heuristic methods such as GA, Differential Evolution (DE) algorithm and PSO (Basturk and Karaboga, 2006; Karaboga and Basturk, 2008). The ABC algorithm has the advantages of strong robustness, fast convergence and high flexibility, fewer control parameters and also it can be used for solving multidimensional and multimodal optimization problems (Karaboga and Basturk, 2007; Ercin and Coban, 2012).

This study, proposes a method to select appropriate weighting matrices for an LQR controller to stabilize cart position and pole angle of a nonlinear inverted pendulum system with DC motor while minimizing settling time, steady state error and overshoot percentage of the output signal as position of the cart. The ABC algorithm is employed to determine weighting matrices.

The thesis has been divided into 8 chapters. Chapter 1 introduces to the topic and outlines the objectives of the study. In Chapter 2, dynamics and mathematical model of inverted pendulum have been presented. In Chapter 3, inverted pendulum system with DC motor has been covered. This chapter explains the mathematical model of DC motor as whole electromechanical system which consists of electrical motor, pulley, and belt, and how it can be combined with inverted pendulum system. In Chapter 4, the basics of the LQR have been explained. In Chapter 5, the ABC algorithm has been presented. In Chapter 6, LQR controller design has been

described. This chapter considers how the ABC algorithm has been applied to the LQR controller design. In the last two chapters, case studies carried out during the study, and the results obtained from them have been presented. In Chapter 7, simulation results of the study have been presented. This chapter describes the simulation setup and shows the simulation results which presented as figures. Additionally, results obtained for proposed method has been compared with a method proposed by Ghosh et al. (2012) and results of comparison presented as figures and tabulated data.

Conclusion of the thesis and future work are presented in Chapter 8.

2. INVERTED PENDULUM

Generally, an inverted pendulum system consists of a cart and a rod hinged it. The cart is moved by a DC motor. The DC motor supplies some force needed for motion of the cart via a pulley-belt mechanism. Dynamics of the inverted pendulum system can be represented as a set of equations which is called mathematical model. Either this model can be represented in transfer function form or state space form. In this chapter the complete mathematical model of the inverted pendulum system has been analysed and then its linearized model has been presented in state space form.

2.1. Dynamics of Inverted Pendulum

The complete mathematical model of the inverted pendulum can be derived from the Newton's laws of motion according to its movement characteristics. The motion of the inverted pendulum system consists of the linear motion of the motor driven cart in the X-axis and the rotational motion of the pendulum in the X-Y plane. Hence there will be two dynamic equations.

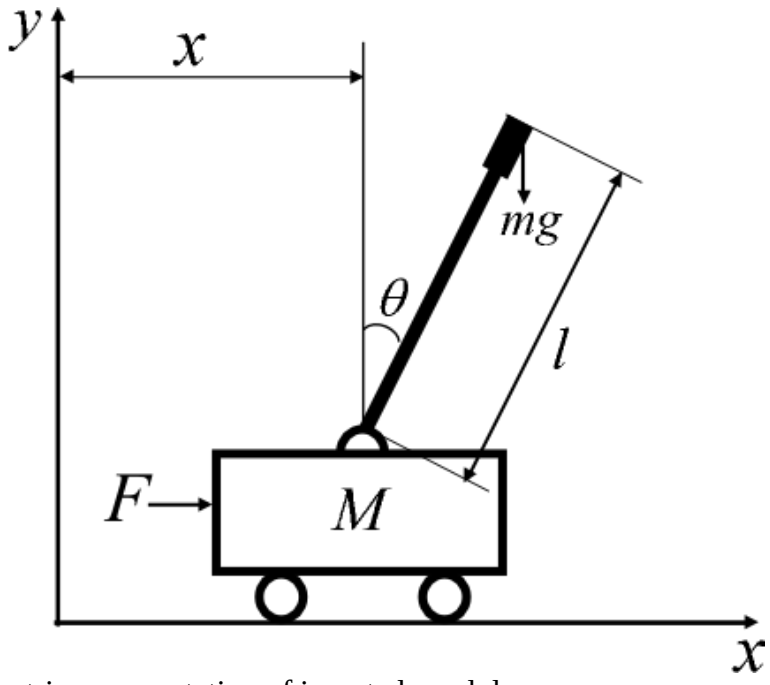

Figure 2.1.Parametric representation of inverted pendulum

The parametric representation of the inverted pendulum system is shown in Figure 2.1. Let x be the displacement of the cart from the initial position in m; θ the angle between the rod and vertical direction in rad. Also let M be the mass of the cart and m the mass of the pendulum in kg; l the length of pendulum in m; g the acceleration due to gravity in m/s^2. F is the force applied to the cart in N. Beside these parameters, b is the cart friction coefficient in Ns/m; J_p is the moment of inertia of pendulum in kg/s^2 and d is the pendulum damping coefficient in Nms/rad which are not shown in Figure 2.1.

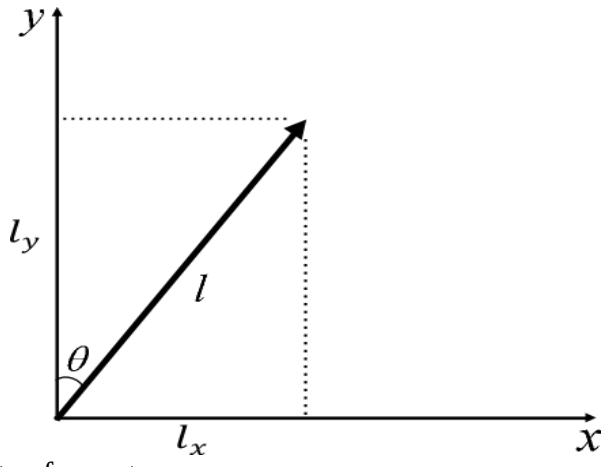

Figure 2.2. Components of a vector

As shown in Figure 2.2 horizontal and vertical components of a vector can be derived as follows:

$$\vec{l}\left(\vec{x},\vec{y},\vec{z}\right)=l_x\vec{x}+l_y\vec{y}+0\vec{z} \tag{2.1}$$

$$\vec{l}=\begin{bmatrix} l_x \\ l_y \\ 0 \end{bmatrix} \tag{2.2}$$

$$l_x=l\sin\left(\theta\right) \tag{2.3}$$

$$l_y = l\cos(\theta) \tag{2.4}$$

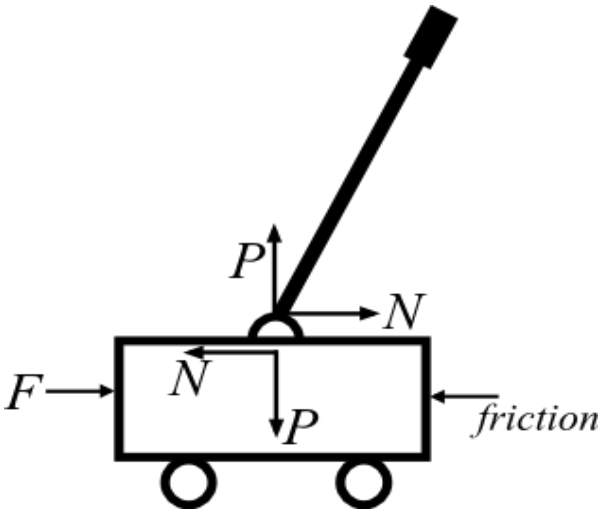

Figure 2.3.Free body diagram of inverted pendulum

Let N be the horizontal component of reaction force and P be the vertical component of the reaction force as shown in Figure (2.3). Define also the coordinates of the centre of gravity of the mass as x_G and y_G. Then considering Figure 2.1 and using Equation (2.3) and Equation (2.4)

$$x_G = x + l_x = x + l\sin(\theta) \tag{2.5}$$

$$y_G = l_y = l\cos(\theta) \tag{2.6}$$

According to the Newton's First Law of Motion, applied force on the cart equals the product of mass and its acceleration.

$$F = ma \tag{2.7}$$

So the horizontal reaction force N becomes:

$$N = m\frac{d^2 x_G}{dt^2}$$

$$N = m\frac{d^2}{dt^2}\left(x + l\sin(\theta)\right) \tag{2.8}$$

Noting that

$$\frac{d}{dt}\sin(\theta) = \cos(\theta)\dot{\theta}$$

$$\frac{d^2}{dt^2}\sin(\theta) = -\sin(\theta)\dot{\theta}^2 + \cos(\theta)\ddot{\theta}$$

$$\frac{d}{dt}\cos(\theta) = -\sin(\theta)\dot{\theta}$$

$$\frac{d^2}{dt^2}\cos(\theta) = -\cos(\theta)\dot{\theta}^2 - \sin(\theta)\ddot{\theta}$$

Equation (2.8) can be rewritten as

$$N = m\left(\ddot{x} + \ddot{\theta}l\cos(\theta) - \dot{\theta}^2 l\sin(\theta)\right) \tag{2.9}$$

The force F applied on the cart equals the sum of the force due to acceleration, friction component of force that opposes the linear motion of the cart and the horizontal reaction.

$$F = M\ddot{x} + b\dot{x} + N \tag{2.10}$$

Substituting Equation (2.9) in Equation (2.10)

$$F = M\ddot{x} + b\dot{x} + m\left(\ddot{x} + \ddot{\theta}l\cos(\theta) - \dot{\theta}^2 l\sin(\theta)\right) \tag{2.11}$$

Equation (2.11) can be rewritten as follows:

$$\mathrm{F} = (M+m)\ddot{x} + b\dot{x} + ml\ddot{\theta}\cos(\theta) - ml\dot{\theta}^2\sin(\theta) \tag{2.12}$$

To get the second equation of motion for inverted pendulum, sum the forces perpendicular to the pendulum. Considering the Figure (2.3) vertical reaction P is given by the weight of the pendulum on the cart. Let $y_G = l\cos\theta$ be the displacement of pendulum from the pivot. Then, P is given by

$$P - mg = m\frac{d^2}{dt^2}\left(l\cos(\theta)\right) \tag{2.13}$$

Equation (2.13) can be rewritten as

$$P = -ml\ddot{\theta}\sin(\theta) - ml\dot{\theta}^2\cos(\theta) + mg \tag{2.14}$$

Noting that the torque equation

$$\vec{\tau} = \vec{l} \otimes \vec{F}$$

where the notation $\otimes$ indicates vector product.

$$\vec{\tau} = \begin{bmatrix} \vec{x} & \vec{y} & \vec{z} \\ l_x & l_y & 0 \\ N & P & 0 \end{bmatrix}$$

$$\vec{\tau} = (-1)^{1+3}\,\vec{z}(\mathrm{P}\,l_x - Nl_y)$$

$$\tau = Pl\sin(\theta) - Nl\cos(\theta) \tag{2.15}$$

Also

$$\tau = J_p\ddot{\theta} + d\dot{\theta} \tag{2.16}$$

where J_p is pendulum moment of inertia and d is pendulum damping coefficient.

Equating Equation (2.15) and Equation (2.16), we can get

$$Pl\sin(\theta) - Nl\cos(\theta) = J_p\ddot{\theta} + d\dot{\theta} \tag{2.17}$$

Substituting Equation (2.9) and Equation (2.14) in Equation (2.17)

$$\begin{aligned} &-ml\ddot{x}\cos(\theta) - ml^2\ddot{\theta}\cos^2(\theta) + ml^2\dot{\theta}^2\sin(\theta)\cos(\theta) \\ &-ml^2\ddot{\theta}\sin^2(\theta) - ml^2\dot{\theta}^2\cos(\theta)\sin(\theta) + mgl\sin(\theta) = J_p\ddot{\theta} + d\dot{\theta} \end{aligned} \tag{2.18}$$

Rearranging Equation (2.18) yields

$$-ml\ddot{x}\cos(\theta) - ml^2\ddot{\theta}\left(\cos^2(\theta) + \sin^2(\theta)\right) + mgl\sin(\theta) = J_p\ddot{\theta} + d\dot{\theta} \tag{2.19}$$

Using the well-known trigonometric equation $\cos^2(\theta) + \sin^2(\theta) = 1$, Equation (2.19) can be rewritten as

$$(J_p + ml^2)\ddot{\theta} - mgl\sin(\theta) + ml\ddot{x}\cos(\theta) + d\dot{\theta} = 0 \tag{2.20}$$

Equation (2.12) and Equation (2.20) are the equations of motion for inverted pendulum that describe the translational and rotational motion, respectively.

2.2. Nonlinear Model of Inverted Pendulum

The equations of motion for inverted pendulum from above can also be represented in state-space form. Therefore the equations can be rearranged into series of first order differential equation.

From Equation (2.12) and Equation (2.20) $\ddot{x}$ and $\ddot{\theta}$ can be shown as, respectively,

$$\ddot{x} = \frac{-b\dot{x} - ml\ddot{\theta}\cos(\theta) + ml\dot{\theta}^2\sin(\theta) + F}{M+m} \tag{2.21}$$

$$\ddot{\theta} = \frac{mgl\sin(\theta) - ml\ddot{x}\cos(\theta) - d\dot{\theta}}{J_p + ml^2} \tag{2.22}$$

Substituting Equation (2.22) into Equation (2.12)

$$\begin{aligned}&(M+m)\ddot{x} + b\dot{x} + ml\left(\frac{mgl\sin(\theta) - ml\ddot{x}\cos(\theta) - d\dot{\theta}}{J_p + ml^2}\right)\cos(\theta)\\ &-ml\dot{\theta}^2\sin(\theta) = F\end{aligned} \tag{2.23}$$

Rearranging Equation (2.23) yields

$$\begin{aligned}&\left(J_p + ml^2\right)(M+m)\ddot{x} + \left(J_p + ml^2\right)b\dot{x}\\ &+ml\cos(\theta)\left(mgl\sin(\theta) - ml\ddot{x}\cos(\theta) - d\dot{\theta}\right)\\ &-\left(J_p + ml^2\right)ml\dot{\theta}^2\sin(\theta) = F\left(J_p + ml^2\right)\end{aligned} \tag{2.24}$$

Collecting $\ddot{x}$ terms on the left-hand-side of Equation (2.24) yields

$$\left(J_p + ml^2\right)(M+m)\ddot{x} - m^2 l^2 \cos^2(\theta)\ddot{x} = -\left(J_p + ml^2\right)b\dot{x} - m^2 l^2 g \cos(\theta)\sin(\theta) + ml\cos(\theta)d\dot{\theta} + ml\dot{\theta}^2 \sin(\theta)\left(J_p + ml^2\right) + F\left(J_p + ml^2\right) \quad (2.25)$$

Equation (2.25) can be rewritten as

$$\ddot{x} = \frac{-\left(J_p + ml^2\right)b\dot{x} - m^2 l^2 g \cos(\theta)\sin(\theta) + ml\cos(\theta)\mathrm{d}\dot{\theta}}{\sigma} + \frac{\left(J_p + ml^2\right)\mathrm{ml}\dot{\theta}^2 \sin(\theta) + \left(J_p + ml^2\right)F}{\sigma} \quad (2.26)$$

where

$$\sigma = \left(J_p + ml^2\right)(M+m) - m^2 l^2 \cos^2(\theta)$$

Similarly substituting Equation (2.21) into Equation (2.22)

$$\left(J_p + ml^2\right)\ddot{\theta} + ml\cos(\theta)\left(\frac{-b\dot{x} - ml\ddot{\theta}\cos(\theta) + ml\dot{\theta}^2\sin(\theta) + F}{M+m}\right) - mgl\sin(\theta) + d\dot{\theta} = 0 \quad (2.27)$$

Rearranging Equation (2.27) yields

$$\left(J_p + ml^2\right)(M+m)\ddot{\theta} - (M+m)mgl\sin(\theta) - ml\cos(\theta)b\dot{x} - m^2 l^2\cos^2(\theta)\ddot{\theta} + m^2 l^2\cos(\theta)\sin(\theta)\dot{\theta}^2 + ml\cos(\theta)F + (M+m)d\dot{\theta} = 0 \quad (2.28)$$

Collecting $\ddot{\theta}$ terms on the left-hand-side in Equation (2.28) yields

$$\left(J_p + ml^2\right)(M+m)\ddot{\theta} - (M+m)mgl\sin(\theta) - ml\cos(\theta)b\dot{x} - m^2l^2\cos^2(\theta)\ddot{\theta}$$
$$-m^2l^2\cos(\theta)\sin(\theta)\dot{\theta}^2 - (M+m)d\dot{\theta} - ml\cos(\theta)F \tag{2.29}$$

Equation (2.29) can be rewritten as

$$\ddot{\theta} = \frac{(M+m)mgl\sin(\theta) + mlb\cos(\theta)\dot{x} - m^2l^2\cos(\theta)\sin(\theta)\dot{\theta}^2}{\sigma} + \frac{-(M+m)d\dot{\theta} - ml\cos(\theta)F}{\sigma} \tag{2.30}$$

Let the states be x, $\dot{x}$, θ and $\dot{\theta}$:

$$\begin{bmatrix} x_1 \\ x_2 \\ x_3 \\ x_4 \end{bmatrix} = \begin{bmatrix} x \\ \dot{x} \\ \theta \\ \dot{\theta} \end{bmatrix}$$

And state equations can be shown as

$$\dot{x}_1 = x_2 \tag{2.31}$$

$$\dot{x}_2 = \frac{-\left(J_p + ml^2\right)bx_2 - m^2l^2g\sin(x_3)\cos(\mathrm{x}_3) + mldx_4\cos(\mathrm{x}_3)}{\sigma} + \frac{\left(J_p + ml^2\right)mlx_4^2\sin(x_3) + \left(J_p + ml^2\right)F}{\sigma} \tag{2.32}$$

$$\dot{x}_3 = x_4 \tag{2.33}$$

$$\dot{x}_4 = \frac{(M+m)mgl\sin(x_3) - m^2l^2\cos(x_3)\sin(x_3)x_4^2}{\sigma} + \frac{+mlb\cos(x_3)x_2 - (M+m)dx_4 - ml\cos(x_3)F}{\sigma} \tag{2.34}$$

2.3. Linear Model of Inverted Pendulum

Since the main aim of this thesis is to design a controller to stabilize the pendulum so as to keep pendulum upright position in response to changes in cart position, linearization of the equations about the vertically upward equilibrium position, $\theta = 0$, is needed. So, assume that very small deviation θ from equilibrium:

$$\theta = 0$$
$$\sin(\theta) = \theta$$
$$\cos(\theta) = 1$$
$$\dot{\theta}^2 = 0$$

Linearization from Equation (2.31) to Equation (2.34) about $\theta = 0$ can be carried out as follows:

$$\dot{x}_1 = x_2 \tag{2.35}$$

$$\dot{x}_2 = \frac{-(J_p + ml^2)bx_2 - m^2l^2g\,x_3 + mldx_4}{\bar{\sigma}} + \frac{(J_p + ml^2)F}{\bar{\sigma}} \tag{2.36}$$

$$\dot{x}_3 = x_4 \tag{2.37}$$

$$\dot{x}_4 = \frac{(M+m)mglx_3 + mlbx_2 - (M+m)dx_4}{\bar{\sigma}} + \frac{-mlF}{\bar{\sigma}} \tag{2.38}$$

where

$$\bar{\sigma} = \left(J_p + ml^2\right)\left(M+m\right) - m^2l^2 = J_p\left(M+m\right) + Mml^2$$

The state-space representation of the linear inverted pendulum is obtained as

$$\begin{bmatrix} \dot{x}_1 \\ \dot{x}_2 \\ \dot{x}_3 \\ \dot{x}_4 \end{bmatrix} = \begin{bmatrix} 0 & 1 & 0 & 0 \\ 0 & \dfrac{-\left(J_p + ml^2\right)b}{\bar{\sigma}} & \dfrac{-m^2l^2g}{\bar{\sigma}} & \dfrac{mld}{\bar{\sigma}} \\ 0 & 0 & 0 & 1 \\ 0 & \dfrac{mlb}{\bar{\sigma}} & \dfrac{\left(M+m\right)mgl}{\bar{\sigma}} & \dfrac{-\left(M+m\right)d}{\bar{\sigma}} \end{bmatrix} \begin{bmatrix} x_1 \\ x_2 \\ x_3 \\ x_4 \end{bmatrix} + \begin{bmatrix} 0 \\ \dfrac{\left(J_p + ml^2\right)}{\bar{\sigma}} \\ 0 \\ \dfrac{-ml}{\bar{\sigma}} \end{bmatrix} F \tag{2.39}$$

$$y = \begin{bmatrix} 1 & 0 & 0 & 0 \\ 0 & 0 & 1 & 0 \end{bmatrix} \begin{bmatrix} x_1 \\ x_2 \\ x_3 \\ x_4 \end{bmatrix} \tag{2.40}$$

3. INVERTED PENDULUM SYSTEM WITH DC MOTOR

In the inverted pendulum system, the cart is driven by a DC motor. To create a more realistic model, the motor characteristics should be added to mathematical model of inverted pendulum system. In this chapter the mathematical model of DC motor has been analysed and then it has been applied to inverted pendulum model.

3.1. DC Motor Model

A motor is an electromechanical component that gives a movement output for a voltage input. That is a mechanical output generated by an electrical input (Nise, 2009). In this section, the transfer function is derived for a particular kind of electromechanical system called armature-controlled DC servomotor (Mablekos, 1980). The motor's schematic diagram and the derived transfer function are shown in Figure 3.1 and Figure 3.2, respectively.

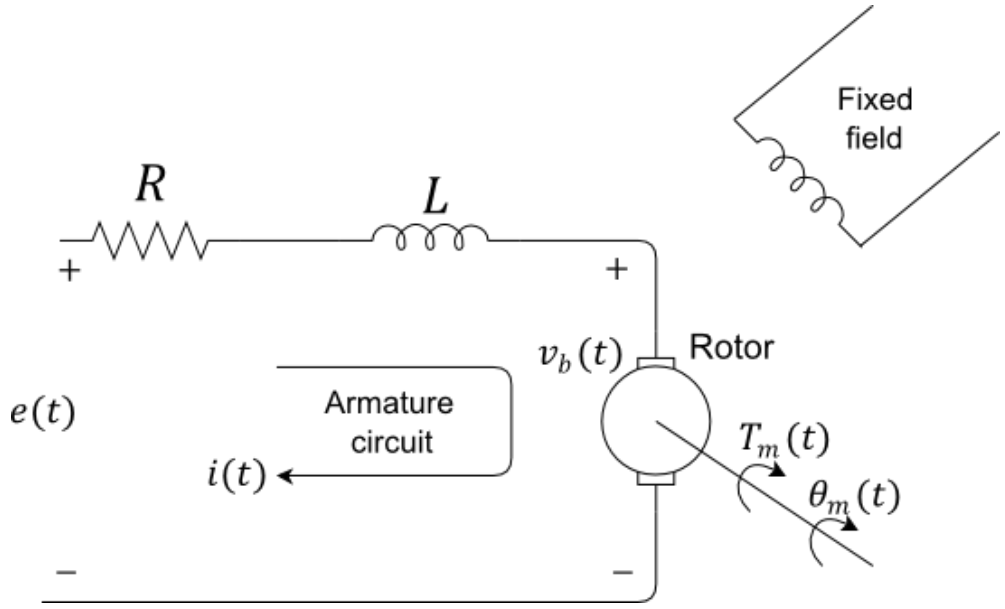

Figure 3.1. DC motor schematic diagram

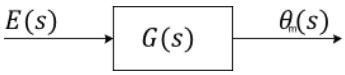

Figure 3.2. DC motor block diagram

In Figure 3.1, the fixed field stands for a magnetic field which is developed by stationary permanent magnets or a stationary electromagnet and armature stands for a rotating circuit which current $i(t)$ flows through magnetic field and feels a force. The resulting torque turns the rotating member of the motor, rotor.

A conductor moving at right angles to a magnetic field generates voltage at the terminals of the conductor equal to $e = Bl_c v$, where e is the voltage, B is the magnetic field flux density, l_c is the length of the conductor, and v is the velocity of the conductor normal to the magnetic field. Since the current-carrying armature is rotating in a magnetic field, its voltage is proportional to speed and named as back electromotive force. Thus,

$$v_b(t) = K_b \frac{d\theta_m(t)}{dt} \tag{3.1}$$

where K_b is back electromotive force constant and $d\theta_m(t)/dt = \omega(t)$ is the angular velocity of the motor. Taking the Laplace transform of Equation (3.1) gives

$$V_b(s) = K_b s\theta_m(s) \tag{3.2}$$

The relation $v_b(t)$ between the armature current $i(t)$ and the applied armature voltage $e(t)$ can be shown by writing a loop equation around the Laplace transformed armature circuit.

$$RI(s) + LsI(s) + V_b(s) = E(s) \tag{3.3}$$

where R and L are rotor circuit resistance and rotor circuit inductance, respectively.

The torque developed by the motor is proportional to the armature current:

$$T_m(s) = K_t I(s) \tag{3.4}$$

where T_m is the torque, and K_t is torque constant, which depends on the motor and magnetic field characteristics.

Rearranging Equation (3.4)

$$I(s) = \frac{1}{K_t} T_m(s) \tag{3.5}$$

Substituting Equation (3.2) and Equation (3.5) into Equation (3.3)

$$\frac{(R+Ls)T_m(s)}{K_t} + K_b s\theta_m(s) = E(s) \tag{3.6}$$

The torque developed by the motor is proportional to the armature current and also can be written as follows:

$$T_m(s) = (J_m s^2 + Ds)\theta_m(s) \tag{3.7}$$

where J_m is the inertia of the motor and, D is the viscous damping.

Substituting Equation (3.7) into Equation (3.6) yields

$$\frac{(R+Ls)(J_m s^2 + Ds)\theta_m(s)}{K_t} + K_b \theta_m s(s) = E(s) \tag{3.8}$$

Equation (3.8) can be rewritten as

$$\frac{\theta_m(s)}{E(s)} = \frac{K_t}{(R+Ls)\left(J_m s^2 + Ds\right) + K_b K_t s} \tag{3.9}$$

Equation (3.9) is the transfer function of the DC motor between the input (voltage) and the output (angular position).

Noting that

$$\omega(s) = \frac{d\theta}{dt} = s\theta(s)$$

$$\theta(s) = \frac{\omega(s)}{s}$$

Substituting $\frac{\omega(s)}{s}$ instead of $\theta(s)$ into Equation (3.9) and Equation (3.6) yields, respectively:

$$\frac{\omega(s)}{E(s)} = \frac{K_t}{(R+Ls)(J_m s + D) + K_b K_t} \tag{3.10}$$

$$\frac{(R+Ls)T_m(s)}{K_t} + K_b\omega(s) = E(s) \tag{3.11}$$

In order to obtain torque developed by the motor and to get rid of angular velocity, substitute $\omega(s)$ from Equation (3.10) into Equation (3.11)

$$\frac{(R+Ls)T_m(s)}{K_t} + K_b\left(\frac{K_t}{(R+Ls)(J_m s + D) + K_b K_t}\right)E(s) = E(s) \tag{3.12}$$

Collecting $E(s)$ terms on the right-hand-side in Equation (3.12) yields

$$\frac{R+Ls}{K_t}T_m(s)=E(s)-\frac{K_bK_t}{(R+Ls)(J_ms+D)+K_bK_t}E(s) \tag{3.13}$$

Rearranging Equation (3.13) yields

$$\frac{R+Ls}{K_t}T_m(s)=\left(1-\frac{K_bK_t}{(R+Ls)(J_ms+D)+K_bK_t}\right)E(s) \tag{3.14}$$

Equation (3.14) can be rewritten as

$$T_m(s)=\frac{K_t}{R+Ls}\left(1-\frac{K_bK_t}{(R+Ls)(J_ms+D)+K_bK_t}\right)E(s) \tag{3.15}$$

Equation (3.15) is the motor torque equation without angular velocity $\omega(s)$ in the equation.

Now let us obtain the force equation induced by the motor torque:

$$\left.\begin{aligned} T_m &= F\frac{\rho}{n_1} \\ F &= \frac{n_1}{\rho}T_m \end{aligned}\right\} \tag{3.16}$$

where ρ and n_1 are radius of pulley and gear ratio, respectively.

Substituting Equation (3.16) into Equation (3.15)

$$F(s)=\left(\frac{n_1}{\rho}\right)\frac{K_t}{R+Ls}\left(1-\frac{K_bK_t}{(R+Ls)(J_ms+D)+K_bK_t}\right)E(s) \tag{3.17}$$

Equation (3.17) can be rewritten by taking into account the tuning gain of DC motor, K_g

$$F(s) = K_g \left(\frac{n_1}{\rho} \right) \frac{K_t}{R + Ls} \left(1 - \frac{K_b K_t}{(R + Ls)(J_m s + D) + K_b K_t} \right) E(s) \tag{3.18}$$

At this point, the effect of motor inductance L on DC motor system is observed by a simulation which examines step response changes on DC motor system by different L values. Simulation parameters are given in Table 3.1, and simulation results for $T = 0.1\text{sec}$ are shown in Figure 3.3. In this simulation we can see the response of force F induced by the DC motor to input voltage. According to the simulation results L has a limited effect on the system at least for simulation purposes, so it is possible to take $L = 0$ for transfer function. However, in practical studies it should be taken into consideration.

Table 3.1. Simulation parameters for force induced by DC motor (Feedback Instruments, 2006)

Parameter	**Value**
$J_m(\text{kgm}^2)$	0.000014
D(Nsec/ m)	0.000001
$\rho(m)$	0.0314
$R(\Omega)$	2.5
K_t	0.05
K_b	0.05
K_g	-9.6
n_1	0.9860
L(H)	0.0025

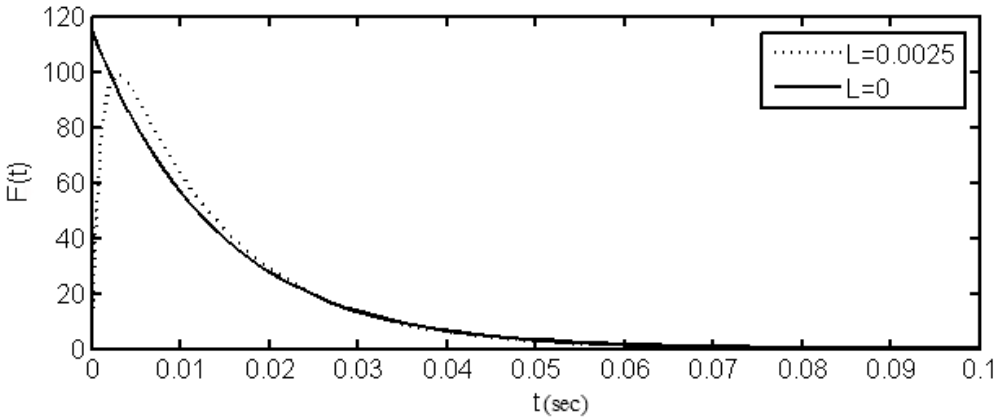

Figure 3.3. Simulation results for force F induced by DC motor

In place of force F in the inverted pendulum equations of motion let us use DC motor armature voltage $E(s)$ as input. Towards this end, rearranging Equation (3.11)

$$T_m(s) = -\frac{K_b K_t}{R+Ls}\omega(s) + \frac{K_t}{R+Ls}E(s) \tag{3.19}$$

Let us write torque – force equation and translational velocity – angular velocity equation, respectively:

$$T_m(s) = F(s)\frac{\rho}{n_1} \tag{3.20}$$

$$\omega(t) = \left(\frac{n_2}{\rho}\right)\frac{dx(t)}{dt} \tag{3.21}$$

where n_2 is gear ratio. Taking Laplace transform of both sides of the Equation (3.21) yields

$$\omega(s) = \left(\frac{n_2}{\rho}\right)sx(s) \tag{3.22}$$

Using Equation (3.19), and Equation (3.20), the force is written in the following equation:

$$F(s) = -\left(\frac{n_1}{\rho}\right)\frac{K_b K_t}{R+Ls}\omega(s) + \left(\frac{n_1}{\rho}\right)\frac{K_t}{R+Ls}E(s) \tag{3.23}$$

Substituting Equation (3.22) into Equation (3.23), the force can be rewritten as follows:

$$F(s) = -\left(\frac{n_1}{\rho}\right)\left(\frac{n_2}{\rho}\right)\frac{K_b K_t}{R+Ls}sx(s) + \left(\frac{n_1}{\rho}\right)\frac{K_t}{R+Ls}E(s) \tag{3.24}$$

For simplification, substituting $L = 0$ in Equation (3.24), we can get

$$F(s) = -\left(\frac{n_1}{\rho}\right)\left(\frac{n_2}{\rho}\right)\frac{K_b K_t}{R}sx(s) + \left(\frac{n_1}{\rho}\right)\frac{K_t}{R}E(s) \tag{3.25}$$

Taking the inverse Laplace transform of Equation (3.25), we can obtain a differential equation whose inputs are motor armature voltage $e(t)$ and translational velocity of the cart $\dot{x}(t)$, and output is the force $F(t)$ applied on the cart. Therefore, with Equation (3.26) electromechanical signal conversation from voltage to force is achieved.

$$F(t) = -\left(\frac{n_1}{\rho}\right)\left(\frac{n_2}{\rho}\right)\frac{K_b K_t}{R}\dot{x}(t) + \left(\frac{n_1}{\rho}\right)\frac{K_t}{R}e(t) \tag{3.26}$$

3.2. Inverted Pendulum Model with DC Motor

x_1, x_2, x_3 and x_4 are the state variables of the inverted pendulum which include force F as input, Equation (2.31) trough Equation (2.34) can be rearranged by substituting Equation (3.26) into them.

$$\dot{x}_1 = x_2 \tag{3.27}$$

$$\dot{x}_2 = \frac{-\left(J_p + ml^2\right)\left(b + \left(\frac{n_1}{\rho}\right)\left(\frac{n_2}{\rho}\right)\frac{K_b K_t}{R}\right)x_2 - m^2 l^2 g \sin\left(x_3\right)\cos\left(\mathrm{x}_3\right)}{\sigma} + \frac{mldx_4 \cos\left(\mathrm{x}_3\right) + \left(J_p + ml^2\right)mlx_4^2 \sin\left(x_3\right) + \left(J_p + ml^2\right)\left(\left(\frac{n_1}{\rho}\right)\frac{K_t}{R}\right)e}{\sigma} \tag{3.28}$$

$$\dot{x}_3 = x_4 \tag{3.29}$$

$$\dot{x}_4 = \frac{\left(M + m\right)mgl \sin\left(x_3\right) + ml\cos\left(x_3\right)\left(b + \left(\frac{n_1}{\rho}\right)\left(\frac{n_2}{\rho}\right)\frac{K_b K_t}{R}\right)\left(x_2\right)}{\sigma} + \frac{-m^2 l^2 \cos\left(x_3\right)\sin\left(\mathrm{x}_3\right)x_4^2 - \left(M + m\right)dx_4 - ml\cos\left(x_3\right)\left(\frac{n_1}{\rho}\frac{K_t}{R}\right)e}{\sigma} \tag{3.30}$$

where

$$\sigma = \left(J_p + ml^2\right)\left(M + m\right) - m^2 l^2 \cos^2\left(\theta\right)$$

Linearizing the state equations given Equation (3.27) through Equation (3.30) as described in Section 2.3 yields

$$\dot{x}_1 = x_2 \tag{3.31}$$

$$\dot{x}_2 = \frac{-\left(J_p + ml^2\right)\left(b + \left(\frac{n_1}{\rho}\right)\left(\frac{n_2}{\rho}\right)\frac{K_b K_t}{R}\right)x_2 - m^2 l^2 g\, x_3 + mldx_4}{\bar{\sigma}} + \frac{\left(J_p + ml^2\right)\left(\left(\frac{n_1}{\rho}\right)\frac{K_t}{R}\right)e}{\bar{\sigma}} \tag{3.32}$$

$$\dot{x}_3 = x_4 \tag{3.33}$$

$$\dot{x}_4 = \frac{\left(M+m\right)mglx_3 + ml\left(b + \left(\frac{n_1}{\rho}\right)\left(\frac{n_2}{\rho}\right)\frac{K_b K_t}{R}\right)x_2 - \left(M+m\right)dx_4}{\bar{\sigma}} + \frac{-ml\left(\left(\frac{n_1}{\rho}\right)\frac{K_t}{R}\right)E}{\bar{\sigma}} \tag{3.34}$$

where

$$\bar{\sigma} = J_p\left(M+m\right) + Mml^2$$

The state-space representation of the linear inverted pendulum with DC motor is obtained as

$$\begin{bmatrix} \dot{x}_1 \\ \dot{x}_2 \\ \dot{x}_3 \\ \dot{x}_4 \end{bmatrix} = \begin{bmatrix} 0 & 1 & 0 & 0 \\ 0 & \frac{-\left(J_p + ml^2\right)\left(b + \left(\frac{n_1}{\rho}\right)\left(\frac{n_2}{\rho}\right)\frac{K_b K_t}{R}\right)}{\bar{\sigma}} & \frac{-m^2 l^2 g}{\bar{\sigma}} & \frac{mld}{\bar{\sigma}} \\ 0 & 0 & 0 & 1 \\ 0 & \frac{ml\left(b + \left(\frac{n_1}{\rho}\right)\left(\frac{n_2}{\rho}\right)\frac{K_b K_t}{R}\right)}{\bar{\sigma}} & \frac{\left(M+m\right)mgl}{\bar{\sigma}} & \frac{-\left(M+m\right)d}{\bar{\sigma}} \end{bmatrix} \begin{bmatrix} x_1 \\ x_2 \\ x_3 \\ x_4 \end{bmatrix}$$

$$+\begin{bmatrix} 0 \\ \dfrac{\left(J_p + ml^2\right)\left(\left(\dfrac{n_1}{\rho}\right)\dfrac{K_t}{R}\right)}{\bar{\sigma}} \\ 0 \\ \dfrac{-ml\left(\left(\dfrac{n_1}{\rho}\right)\dfrac{K_t}{R}\right)}{\bar{\sigma}} \end{bmatrix} e \tag{3.35}$$

$$y = \begin{bmatrix} 1 & 0 & 0 & 0 \\ 0 & 0 & 1 & 0 \end{bmatrix} \begin{bmatrix} x_1 \\ x_2 \\ x_3 \\ x_4 \end{bmatrix} \tag{3.36}$$

4. LINEAR QUADRATIC REGULATOR

The state space representation of a linear time-invariant (LTI) continuous time control system can be written as follows (Ogata, 1995):

$$\left.\begin{aligned} \dot{x} &= Ax + Bu \\ y &= Cx \end{aligned}\right\} \tag{4.1}$$

where x is state vector (n vector) and u is control vector (r vector), respectively. A and B are $n \times n$ and $n \times r$ constant matrices, indicating system.

If all states are available for feedback and states are controllable then there is a feedback gain matrix K of the optimal control vector

$$u(t) = -Kx(t) \tag{4.2}$$

Linear quadratic optimal control problem may be stated to find the optimal input u sequence that minimizes the quadratic performance index which is defined as:

$$J = \int_0^\infty (x^T Q x + u^T R u) dt \tag{4.3}$$

where Q is an $n \times n$ positive semi-definite or positive definite real symmetric matrix and R is an $r \times r$ positive definite real symmetric matrix (Ogata, 1995). The superscript (T) indicates transpose of a matrix.

Noting that $u^T R u$ term of Equation (4.3) accounts for the expenditure of the energy of control signals. The matrices Q and R determine the relative importance of the error and the expenditure of this energy.

The block diagram showing the optimal configuration of quadratic optimal regulator is shown in Figure 4.1. If the unknown elements of the matrix K are

determined so as to minimize the performance index, then $u(t) = -Kx(t)$ is optimal for any initial state $x(0)$.

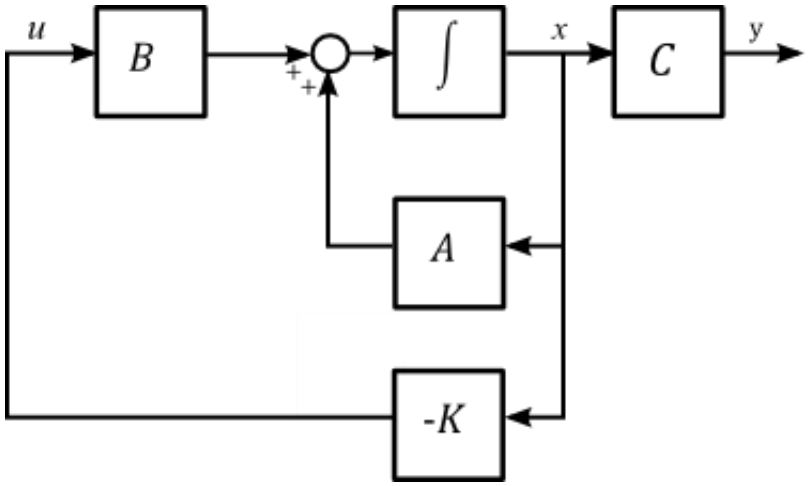

Figure 4.1. Optimal regulator system

To solve the optimization problem, substituting Equation (4.2) into Equation (4.1) yields

$$\dot{x} = Ax - BKx = (A - BK)x \tag{4.4}$$

In the following derivations, it is assumed that the matrix $(A - BK)$ is stable, or that the eigenvalues of the matrix $(A - BK)$ have negative real parts.

Substituting Equation (4.2) into Equation (4.3) yields (Ogata, 1995)

$$J = \int_0^\infty \left(x^T Q x + x^T K^T R K x \right) dt \tag{4.5}$$

or

$$J = \int_0^\infty x^T \left(Q + K^T R K \right) x dt \tag{4.6}$$

Setting

$$x^T\left(Q+K^TRK\right)x=-\frac{d}{dt}\left(x^TPx\right) \tag{4.7}$$

where P is a positive definite real symmetric matrix.

Taking the derivative of the right hand side of Equation (4.7) yields

$$x^T\left(Q+K^TRK\right)x=-\dot{x}^TPx-x^TP\dot{x} \tag{4.8}$$

Substituting Equation (4.4) in Equation (4.8)

$$x^T\left(Q+K^TRK\right)x=-x^T\left[\left(A-BK\right)^TP+P\left(A-BK\right)\right]x \tag{4.9}$$

Noting that Equation (4.9) must hold true for any x and comparing both sides of this equation require that (Ogata, 1995)

$$\left(A-BK\right)^TP+P\left(A-BK\right)=-\left(Q+K^TRK\right) \tag{4.10}$$

Using Equation (4.7), Equation (4.6) can be written as

$$J=\int_0^\infty -\frac{d}{dt}\left(x^TPx\right)dx=-x^TPx\Big|_0^\infty \tag{4.11}$$

$$J=-x^T\left(\infty\right)Px\left(\infty\right)+x^T\left(0\right)Px\left(0\right) \tag{4.12}$$

Since all eigenvalues of $\left(A-BK\right)$ are assumed to have negative real parts, $x\left(\infty\right)\to 0$. Therefore, Equation (4.12) becomes

$$J=x^T\left(0\right)Px\left(0\right) \tag{4.13}$$

Thus, the performance index J can be obtained in terms of the initial condition $x(0)$ and P.

Since R matrix is assumed to be a positive definite real symmetric matrix, it can be written as

$$R = T^T T \tag{4.14}$$

where T is a non-singular matrix. Substituting Equation (4.14) into Equation (4.10) yields (Ogata, 1995)

$$\left(A^T - K^T B^T\right)P + P\left(A - BK\right) + Q + K^T T^T TK = 0 \tag{4.15}$$

which can be rewritten as

$$A^T P + PA + \left[TK - \left(T^T\right)^{-1} B^T P\right]^T \left[TK - \left(T^T\right)^{-1} B^T P\right] - PBR^{-1}B^T P + Q = 0 \tag{4.16}$$

The minimization of J with respect to K requires the minimization of

$$x^T \left[TK - \left(T^T\right)^{-1} B^T P\right]^T \left[TK - \left(T^T\right)^{-1} B^T P\right] x$$

with the respect to K. Since this expression is nonnegative, the minimum occurs when it is zero, or when

$$TK - \left(T^T\right)^{-1} B^T P = 0 \tag{4.17}$$

Hence,

$$K = T^{-1}\left(T^T\right)^{-1} B^T P \tag{4.18}$$

Substituting Equation (4.14) for R into Equation (4.18) we can get

$$K = R^{-1}B^T P \tag{4.19}$$

Equation (4.19) gives the optimal gain matrix K. Thus, the optimal control law to the quadratic optimal control problem when the performance index is given by Equation (4.3) is linear and is given by

$$u(t) = -Kx(t) \tag{4.20}$$

The matrix P in Equation (4.19) must satisfy Equation (4.10) or the following reduced equation which is called the reduced-matrix Ricatti equation is obtained from Equation (4.16) for minimum $TK - \left(T^T\right)^{-1} B^T P = 0$:

$$A^T P + PA - PBR^{-1}B^T P + Q = 0 \tag{4.21}$$

In order to obtain the feedback gain matrix K first Equation (4.21) must be solved for the matrix P then it is substituted in Equation (4.19).

5. ARTIFICIAL BEE COLONY ALGORITHM

Colonies of the social insects such as bees, ants, and fish have the instinctive ability behave collectively to solve problems further with help of the capability of individuals. This ability is called as swarm intelligence. For example, food sources or environmental threats discovered by individuals can be spread quickly in the hive through the interaction with other individuals. In this way, the common reaction being supposed to be given can be an example of the intelligent behaviour of colony in a collective structure. Such colonies are characterized by self-organization, adaptiveness and robustness (Bonebeau et al., 1999; Bonebeau and Meyer, 2001).

A mathematical model of foraging behaviour of a honey bee colony based on reaction–diffusion equations was developed by Tereshko (2000). The model has three fundamental parts: food sources, employed foragers, and unemployed foragers. Food sources are defined as a number of properties such as taste of nectar, closeness to the hive and nectar amount, and a forger bee evaluates these properties to choose a food source. An employed forager carries information about a specific food source and shares it with other bees. An unemployed forager looks for a food source to exploit it. Also two main mechanism of the honey bee colony behaviour are defined as recruitment to a food source and abandonment of a food source by this model (Tereskho, 2000).

The Artificial Bee Colony (ABC) algorithm was introduced by Karaboga (2005) in Turkey as a new optimization method in the field of swarm intelligence. The ABC algorithm is based on the intelligent behaviour of honey bee swarms finding food sources to optimize numerical functions. Also the ABC algorithm can be used for solving multidimensional and multimodal optimization problems (Karaboga and Basturk, 2007).

In the ABC algorithm, the colony contains three groups of bees: employed, onlooker, and scout. An employed bee goes to a food source to collect nectar and provides information about the food source. An onlooker bee gets the information about food sources from employed bees and chooses a food source. A scout bee searches new food sources randomly. There is only one employed bee in the colony

for every food source. So the number of the employed bees is equal to the food sources around the hive. Also the number of the employed bees is equal to the number of the onlooker bees. If an employed bee abandons its food source, it becomes a scout bee (Akay and Karaboga, 2009a, 2009b).

At the beginning of the process, bees select a set of food source positions randomly and determine the nectar amounts of the selected food sources in the ABC algorithm. Then, these bees return the hive and share the information with the other bees, waiting on the dance area. After sharing the information employed bees return to the food source which selected by themselves. If an employed bee consumes the food source, starts to look for another source in the neighbourhood of the previous one. Then, an onlooker bee choose a food source depending on the information provided by the employed bees. This division of labour between onlooker bees and employed bees provide the exploitation of local sources and scout bees provide the exploration of new sources. The main steps of the ABC algorithm are given below (Karaboga and Basturk, 2007):

1:Initialize Population
*2:**repeat***
3:Place the employed bees on their food sources
4:Place the onlooker bees on the food sources depending on their nectar amounts
5:Send the scouts to the search area for discovering new food sources
6:Memorize the best food source found so far
*7:**until** requirements are met*

The position of a food source is a possible solution of the optimization problem in the ABC algorithm. The quality of the solution depends on the nectar amount of the associated food source. Initial population of food source positions (SN) is generated randomly by the ABC algorithm at the first step. Each food source as a solution $x_i (i = 1, 2, ..., SN)$ is a D_{op}-dimensional vector where D_{op} denotes the

number of the parameters in the optimization problem (Akay and Karaboga, 2009a, 2009b).

After the initialization of the ABC algorithm, all bees search every food source until a predetermined number of iterations $(Cycle = 1, 2, ..., MCN)$, where MCN represents the maximum cycle number. An employed bee produces a modification on the food source for finding a new food source and tests the nectar amount of new food source. If the new nectar amount is higher than the previous one, the position of new sources replaces with the old position. Otherwise, the bee keeps the position of the previous one. After all employed bees complete their search process, the nectar information and positions of the food sources are shared with the onlooker bees. An onlooker bee evaluates the information of nectar amounts of food sources from employed bees then chooses a food source by using a selection probability related to that evaluated information (Akay and Karaboga, 2009a, 2009b).

An onlooker bee chooses a food source depending on the probability value of that food source, p_i, determined by the Equation (5.1) as follows (Akay and Karaboga, 2009a, 2009b):

$$p_i = \frac{fit_i}{\sum_{i=1}^{SN} fit_i} \tag{5.1}$$

where fit_i denotes the fitness value of the solution i and it is proportional to the nectar amount of the food source in the position i.

The ABC algorithm uses the Equation (5.2) to produce a new food position from the old position in the memory (Akay and Karaboga, 2009a, 2009b).

$$v_{ij} = x_{ij} + \phi_{ij}\left(x_{ij} - x_{kj}\right) \tag{5.2}$$

where $j \in \{1,2,...,D_{op}\}$ and $k \in \{1,2,...,SN\}$ are randomly selected indexes. Despite it is determined randomly, the index k should be different from i. ϕ_{ij} is determined in the range of $[-1,1]$ randomly, and controls the production of a food source position around the neighbourhood of x_{ij}. As seen from Equation (5.2), as long as the difference between the parameters x_{ij} and x_{kj} decreases, the perturbation on the position x_{ij} decreases. Hence, as the search comes close to optimum solution in the search space, the step length is adaptively reduced.

The food source is abandoned by the employed bees is replaced with a new food source by scout bees. In the ABC algorithm this is simulated by producing a position randomly and replacing it with the previous one. If a position cannot be improved further during a predetermined number of cycles which is called *limit*, then that food source is thought to be abandoned. After the abandonment of a food source, scout bees discover a new food source to replace with it. This operation can be defined as follows (Akay and Karaboga, 2009a, 2009b):

$$x_i^j = x_{min}^j + rand[0,1]\left(x_{max}^j - x_{min}^j\right) \tag{5.3}$$

where $i \in \{1,2,...,SN\}$ and $j \in \{1,2,...,D_{op}\}$.

After producing and evaluating of each candidate source position v_{ij}, the performance of the candidate source position is compared with the old one. If the nectar amount of new source is equal or better than the nectar amount of the old source, the new source position is replaced with the old one or else the old food position is kept in the memory. So, a greedy selection mechanism is engaged as the selection operation between the candidate food source and the old one (Karaboga and Akay, 2009).

Altogether, ABC algorithm has four different selection processes (Karaboga and Akay, 2009):

1. A global probabilistic selection process for the discovering promising regions by the onlooker bees using the probability value which is determined by Equation (5.1).
2. A local probabilistic selection process to determine a new food source around the old source in the memory using Equation (5.2).
3. A local selection called greedy selection process to determine that if the nectar amount of the candidate source is better than that of the present one.
4. A random selection process as defined in Equation (5.3)

In a robust search process, exploration and exploitation processes have to be performed. In the ABC algorithm exploration process is controlled by scout bees while exploitation process is carried out by onlooker bees and employed bees in the search space. The flowchart of the ABC algorithm is shown in Figure 5.1. Also the detailed pseudo-code of the ABC algorithm is given below (Akay and Karaboga, 2009a, 2009b):

Step 1:*Initialize the population of solutions* x_i , $i = 1,...,SN$

Step 2:*Evaluate the population*

Step 3*:cycle = 1*

Step 4:*repeat*

Step 5:*Produce new solutions* v_i *for the employed bees by using Equation (5.2) and evaluate them*

Step 6:*Apply the greedy selection process for the employed bees*

Step 7:*Calculate the probability values* p_i *for the solutions* x_i *by Equation (5.1)*

Step 8:*Produce the new solutions* v_i *for the onlookers from the solutions* x_i *selected depending on* p_i *and evaluate them*

Step 9: *Apply the greedy selection process for the onlookers*

Step 10:*Determine the abandoned solution for the scout, if exists, and replace it with a new randomly produced solution* x_i *by Equation (5.3)*

Step 11:*Memorize the best solution achieved so far*

Step 12:*cycle = cycle + 1*

Step 13:*until cycle = MCN*

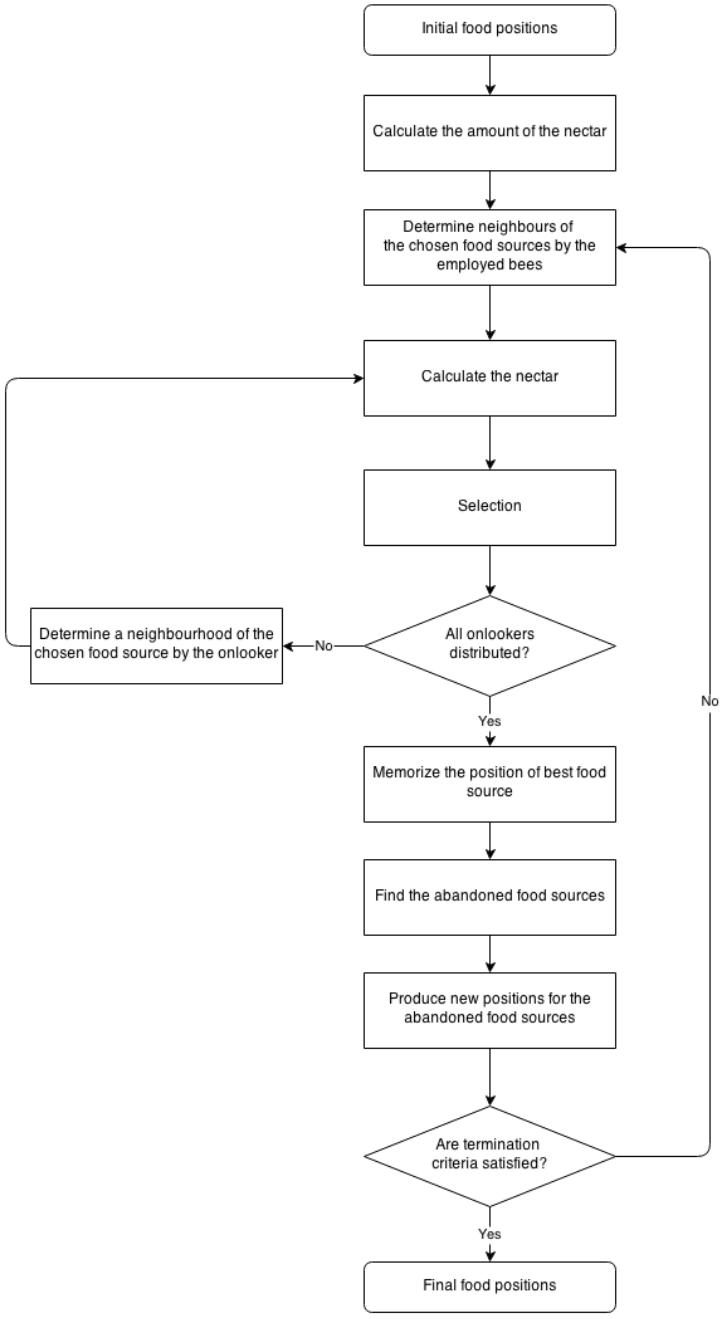

Figure 5.1. Flowchart of the Artificial Bee Colony Algorithm

6. LQR CONTROLLER DESIGN USING THE ABC ALGORITHM

The performance quality of the controller design using LQR method highly depends on the choice of weighting matrices Q and R. Generally, selecting these weights is performed by trial and error method as mentioned before.

In this study the ABC algorithm is employed to select Q and R to design an LQR controller for considering both pendulum's angle and cart's position. In the following sub-sections we shall explain how to determine the matrices Q and R of LQR using the ABC algorithm in order to take time-domain specifications into account.

6.1. Applying the ABC Algorithm in LQR Controller Design

Main design parameters of LQR are weighting matrices. Tuning the parameters of the LQR controller using the ABC algorithm is an optimization problem. This optimization problem needs to be solved in such a way that output of the system attains the desired level in the shortest time as far as possible without a high overshoot. Hence, the goal of this design is to reduce the settling time (t_s) of the output of the system y (the cart position) without overshoot (os) or with minimum overshoot and also minimize steady-state error (e_{ss}). The objective weighting method where multiple objective functions are combined into one objective function f_{sum} can be used for multiple objective optimization (Coban, 2011). The objective function f_{sum} can be defined as

$$f_{sum} = K_1 t_s + K_2 os + K_3 e_{ss} \tag{6.1}$$

where K_1, K_2 and K_3 are weight coefficients of the fitness functions and their values were chosen as 1.0 by trial and error in this study.

In addition to time-domain specifications included in the objective function given in Equation (6.1) important physical constraints of the controlled system should be added to the objective function. The inverted pendulum system has two physical constraints. The first one is the bound of the control signal which must be in the range of -2.5V and +2.5V and the second one is the cart position which is physically bounded by the rail length which is 1 meter. Since, it is assumed that the initial cart position is in the middle of the rail, position of the cart can be limited as $|x| \leq 0.5$ (Feedback Instruments, 2006).

The cart position constraint is already incorporated into the objective function f_{sum} which is given in Equation (6.1), through the overshoot (os), on the other hand, to incorporate the control signal (u) into the ABC algorithm fitness function, a penalty method is used. The objective function given in Equation (6.1) can be evaluated with the proposed method in the following way (Coban, 2011):

$$\text{evaluate } f_{sum} = \begin{cases} f_{sum}, & if \quad |u| \leq 2.5 \\ f_{sum} + \psi, & otherwise \end{cases} \tag{6.2}$$

where ψ denotes a penalty coefficient for violation of the control signal bound. The penalty coefficient ψ is 0 if $|u| \leq 2.5$ otherwise it is a positive constant. In this study ψ is selected as 5.0 by trial and error.

Block diagram of the ABC training is shown in Figure 6.1. The reference input is selected as $r = 0.2$. A pre-compensation scale factor $\bar{N}$ which addresses the steady state error, is added to the reference input as shown in Figure 6.1. Pre-compensation scale factor $\bar{N}$ can be defined as follows (Messner and Tilbury, 2011):

$$\bar{N} = -\left(C_n \left(A - BK\right)^{-1} B\right)^{-1} \tag{6.3}$$

where $C_n = [1\ 0\ 0\ 0]$ to ensure that the reference input will be only applied to the first state which is the position of the cart.

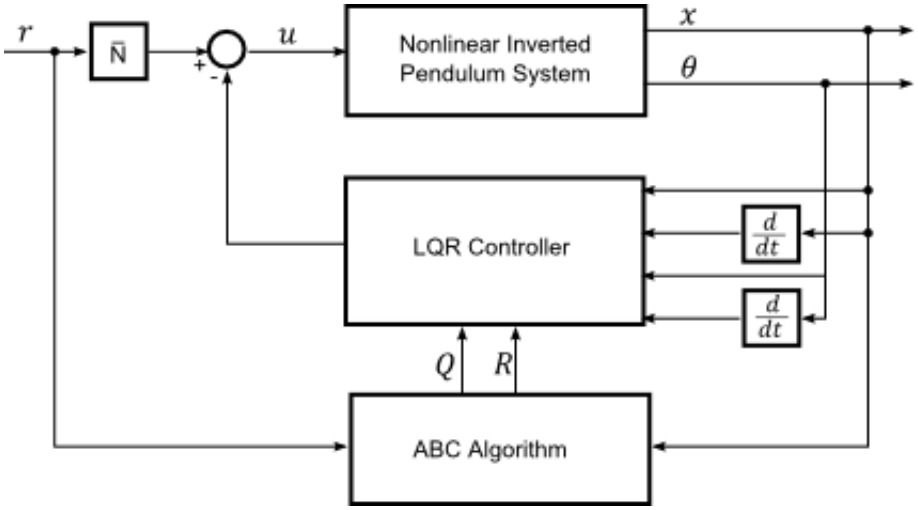

Figure 6.1. Block Diagram of the ABC training

The inverted pendulum system model shown in Figure 6.1 and also the inverted pendulum system model which is used in LQR controller will be described in Section 6.1.2.

6.1.1. Parameters of the ABC Algorithm

As mentioned in the previous sections, Q and R weighting matrices must be real symmetric and positive definite matrices to ensure stability. Also Q and R matrices must be nonnegative definite to ensure $x^T Qx$ and $u^T Ru$ are nonnegative for all possible x and u in Equation (4.3). The easiest way to ensure that the matrices are nonnegative definite is picking the weighting matrices to be diagonal with all diagonal elements positive or zero (Franklin et al., 2006). Hence, weighting matrices are selected as diagonal matrices in literature commonly.

Selecting diagonal weighting matrices causes the interaction of the components of the states and control to decrease. However, this is not unique way to

guarantee the weighting matrices to be positive definite. There exists another way in matrix theory to make sure that a matrix Q being positive definite.

Noting the algebraic principle; a real symmetric matrix Q is positive definite if there exists a non-singular matrix $\bar{Q}$ such that (Ayres, 1962)

$$Q = \bar{Q}\bar{Q}^T \tag{6.4}$$

Since Q matrix is defined in the form $Q = \bar{Q}\bar{Q}^T$ and R matrix $R = \bar{R}\bar{R}^T$, Q and R would be positive definite in any case. In this way we have more degree of freedom to select elements of matrices than diagonal matrices.

Since there is not a direct relation with the matrices' elements and performance specifications, choosing of weighting matrices is not simple. In order to meet these constraints the ABC algorithm was employed to select the best Q and R matrices that minimize the Equation (6.1) in view of the time-domain performance specifications.

The main parameters of the ABC algorithm, colony size and maximum number of cycles are set as $SN = 20$ and $MCN = 100$ by trial and error. To create two matrices which $\bar{Q}$ is 4×4 and $\bar{R}$ is 1×1 non-singular real symmetric matrices, the number of parameters of the problem to be optimized is defined as 11 and they will be denoted as $X_1, X_2, ...\mathrm{X}_{11}$. Also the lower and upper bounds of the parameters are set 0.1 and 5, respectively, by trial and error.

$\bar{Q}$ and $\bar{R}$ matrices are defined as follows.

$$\bar{Q} = \begin{bmatrix} \bar{q}_{11} & \bar{q}_{12} & \bar{q}_{13} & \bar{q}_{14} \\ \bar{q}_{21} & \bar{q}_{22} & \bar{q}_{23} & \bar{q}_{24} \\ \bar{q}_{31} & \bar{q}_{32} & \bar{q}_{33} & \bar{q}_{34} \\ \bar{q}_{41} & \bar{q}_{42} & \bar{q}_{43} & \bar{q}_{44} \end{bmatrix} \tag{6.5}$$

$$\bar{R} = \begin{bmatrix} \bar{r}_{11} \end{bmatrix} \tag{6.6}$$

where

$$\bar{q}_{11} = X_1$$
$$\bar{q}_{12} = \bar{q}_{21} = X_2$$
$$\bar{q}_{13} = \bar{q}_{31} = X_3$$
$$\bar{q}_{14} = \bar{q}_{41} = X_4$$
$$\bar{q}_{22} = X_5$$
$$\bar{q}_{23} = \bar{q}_{32} = X_6$$
$$\bar{q}_{24} = \bar{q}_{42} = X_7$$
$$\bar{q}_{33} = X_8$$
$$\bar{q}_{34} = \bar{q}_{43} = X_9$$
$$\bar{q}_{44} = X_{10}$$
$$\bar{r}_{11} = X_{11}$$

In a consequence, we have 11 parameters $(X_1, X_2, ..., X_{11})$ to be encoded in the ABC algorithm as a solution vector. Hence, the number of optimization parameters $D_{op} = 11$

6.1.2. Inverted Pendulum Models Used for the ABC Algorithm Training

In the ABC algorithm training, the nonlinear model of the inverted pendulum with DC motor given in Equation (3.27) through Equation (3.30) and the linear model of the inverted pendulum with DC motor given in Equation (3.31) through Equation (3.34) are combined to create a more realistic simulation. The system model required to design LQR is linear. Parameters of the DC motor and parameters of the inverted pendulum are presented in Table 6.1 and Table 6.2, respectively.

Table 6.1. Parameters of DC motor (Feedback Instruments, 2006)

Parameter	Value
$R(\Omega)$	2.5
$\rho(m)$	0.0314
K_t	0.05
K_b	0.05
K_g	-9.6
n_1	0.9860
n_2	18.84

Table 6.2. Parameters of Inverted Pendulum (Feedback Instruments, 2006)

Parameter	Value
$M(kg)$	2.3
$m(kg)$	0.2
$l(m)$	0.3
$g(m/s^2)$	9.81
$J_p(kgm^2)$	0.0099
$d(Nms/rad)$	0.005
$b(Ns/m)$	0.00005

The linear model of the inverted pendulum with DC motor given in (3.31) through Equation (3.34) is used to calculate gain matrix K during the training. Substituting the parameters which is given in Table 6.1 and Table 6.2 into Equation (3.35) and Equation (3.36) yields

$$\begin{bmatrix} \dot{x}_1 \\ \dot{x}_2 \\ \dot{x}_3 \\ \dot{x}_4 \end{bmatrix} = \begin{bmatrix} 0 & 1 & 0 & 0 \\ 0 & -76.2828 & -0.5339 & 0.0045 \\ 0 & 0 & 0 & 1 \\ 0 & 164.0490 & 22.2449 & -0.1890 \end{bmatrix} \begin{bmatrix} x_1 \\ x_2 \\ x_3 \\ x_4 \end{bmatrix} + \begin{bmatrix} 0 \\ -48.5878 \\ 0 \\ 104.4898 \end{bmatrix} e \tag{6.7}$$

$$y = \begin{bmatrix} 1 & 0 & 0 & 0 \\ 0 & 0 & 1 & 0 \end{bmatrix} \begin{bmatrix} x_1 \\ x_2 \\ x_3 \\ x_4 \end{bmatrix} \tag{6.8}$$

Since the state-space representation of a continuous time LTI control system can be written as in Equation (4.1), the matrices A , B and C can be defined as follows:

$$\dot{x} = Ax + Bu$$
$$y = Cx$$

where

$$A = \begin{bmatrix} 0 & 1 & 0 & 0 \\ 0 & -76.2828 & -0.5339 & 0.0045 \\ 0 & 0 & 0 & 1 \\ 0 & 164.0490 & 22.2449 & -0.1890 \end{bmatrix}$$

$$B = \begin{bmatrix} 0 \\ -48.5878 \\ 0 \\ 104.4898 \end{bmatrix}$$

$$C = \begin{bmatrix} 1 & 0 & 0 & 0 \\ 0 & 0 & 1 & 0 \end{bmatrix}$$

For general convention we can use the notation u as control instead of input voltage e.

The matrices A and B are used with the weighting matrices Q and R which are selected by the ABC algorithm to calculate gain matrix K.

Since the nonlinear model of the inverted pendulum with DC motor given in Equation (3.27) through Equation (3.30) is used to calculate the objective function f_{sum} during the training, substituting the parameters which is given in Table 6.1 and Table 6.2 into Equation (3.27) through (3.30) yields, respectively,

$$\dot{x}_1 = x_2 \tag{6.9}$$

$$\dot{x}_2 = \frac{-5.0461x_2 - 0.0353\sin(x_3)\cos(x_3) + 0.0003x_4\cos(x_3)}{0.0662\cos^2(x_3)} + \frac{0.0017x_4^2\sin(x_3) - 3.2141u}{0.0662\cos^2(x_3)} \tag{6.10}$$

$$\dot{x}_3 = x_4 \tag{6.11}$$

$$\dot{x}_4 = \frac{1.4715\sin(x_3) + 10.8518\cos(x_3)x_2}{0.0662\cos^2(x_3)} + \frac{-0.0036\cos(x_3)\sin(x_3)x_4^2 - 0.0125x_4 + 6.9120\cos(x_3)u}{0.0662\cos^2(x_3)} \tag{6.12}$$

Equation (6.9) through Equation (6.12) is solved using fourth-order Runge-Kutta method to simulate the nonlinear system and calculate the objective function f_{sum} from the output of the system. The classical fourth-order Runge-Kutta method is a well-known method to solve an ordinary differential equation in a numerical manner.

6.2. The ABC Algorithm Training Results

The inverted pendulum models used in the ABC training has been obtained in previous chapter. The state space representation of inverted pendulum given in Equation (6.7) and Equation (6.8) is used to calculate feedback gain matrix K and pre-compensation scale factor $\bar{N}$, and also the nonlinear model of the pendulum given in Equation (6.9) through Equation (6.12) is used to simulate the inverted pendulum and calculate the object function given in Equation (6.2).

In every cycle of the ABC algorithm, new Q and R matrices are selected and a new feedback gain matrix K is obtained in the following way:

(1) Solving the algebraic Ricatti equation given in Equation (4.21) for P

$$A^T P + PA - PBR^{-1}B^T P + Q = 0$$

where A and B are given in Equation (6.7), Q and R are updated by the ABC algorithm.

(2) Finding the feedback gain matrix using Equation (4.19)

$$K = R^{-1}B^T P$$

Also pre-compensation scale factor $\bar{N}$ is obtained from Equation (6.3). After the calculation of K and $\bar{N}$, results are simulated by using the nonlinear inverted pendulum model as shown in Figure 6.1 and the objective function given in Equation (6.2) is calculated based on the simulation results. The weighting matrices which have provided the best fitness are memorized. The flowchart of the ABC training is shown in Figure 6.2.

The average fitness values during the ABC algorithm training is shown in Figure 6.3. The weighting matrices determined by the ABC algorithm are

$$Q = \begin{bmatrix} 60.1859 & 15.6690 & 46.3669 & 8.9202 \\ 15.6690 & 7.7362 & 15.0121 & 4.4609 \\ 46.3669 & 15.0121 & 41.7765 & 8.4310 \\ 8.9202 & 4.4609 & 8.4310 & 2.5799 \end{bmatrix} \qquad (6.13)$$

$$R = \begin{bmatrix} 0.3941 \end{bmatrix}$$

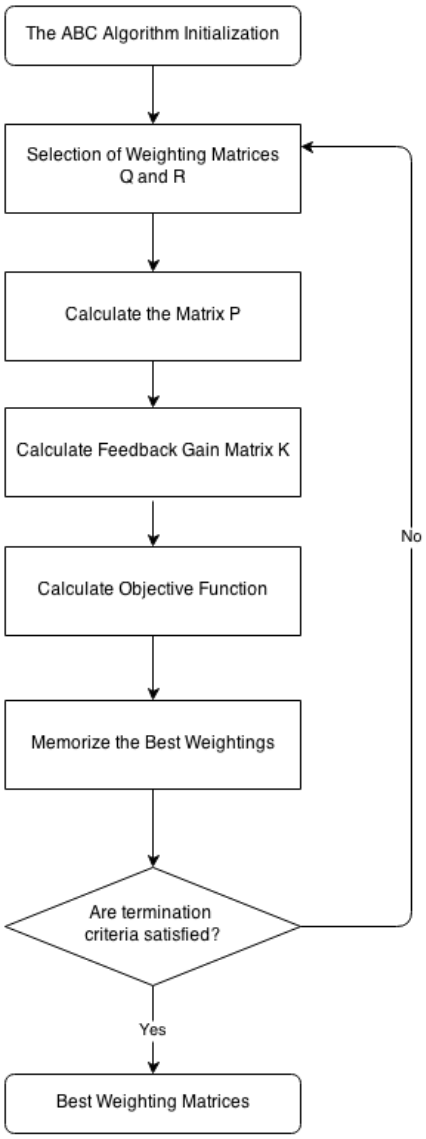

Figure 6.2. Flowchart of the ABC Training

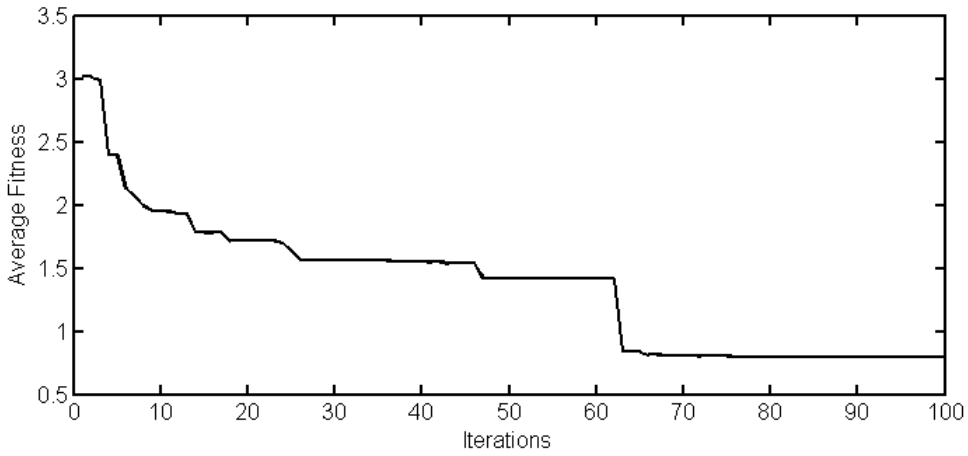

Figure 6.3. Average fitness during the ABC algorithm convergence.

7. SIMULATION RESULTS AND DISCUSSIONS

After the LQR training which is performed so as to determine the matrices Q and R using the ABC algorithm is finished, four different simulations are carried out to investigate the performance of the weighting matrices and these results are compared with a method proposed by Ghosh et al. (2012). The simulation setup, simulation results, and comparison results are presented in the following sub-sections.

7.1. Simulation Setup

Block diagram of the LQR controller of the nonlinear inverted pendulum system with DC motor shown in Figure 7.1 is employed for all the simulation tests. State equations described in Equation (6.9) through Equation (6.12) are used to simulate the nonlinear system. These equations are solved using fourth-order Runge-Kutta method in a numerical manner where the step size $h = 0.001$.

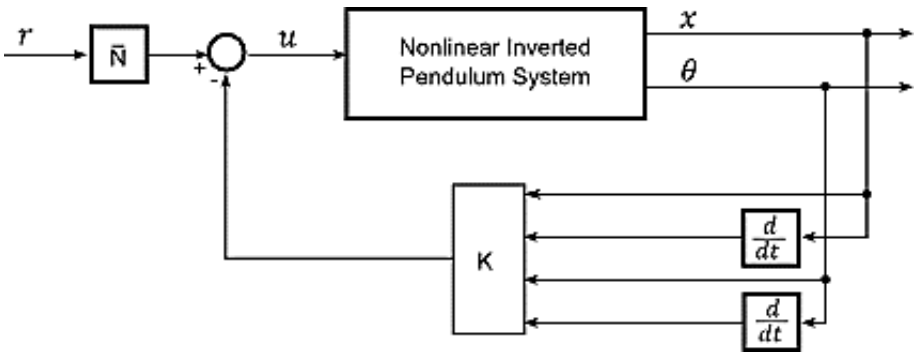

Figure 7.1. Block diagram of the LQR controller for the nonlinear inverted pendulum system with DC motor

To obtain feedback gain matrix K, the algebraic Ricatti equation given in Equation (4.21) is solved for P

$$A^T P + PA - PBR^{-1}B^T P + Q = 0$$

where A and B are given in Equation (6.7), Q and R are given in Equation (6.13). Then using the Equation (4.19), the feedback gain matrix is obtained as

$$K = \begin{bmatrix} 12.3579 & 8.1225 & 18.0051 & 4.0557 \end{bmatrix} \tag{7.1}$$

Using Equation (6.3) and based on K given in Equation (7.1) and matrices A , B and C, scale factor can be determined as

$$\bar{N} = 12.3579 \tag{7.2}$$

7.2. Simulation Results

The goals of these simulations are to show the changes on position of the cart x, pendulum angle θ and control signal u based on initial conditions of $\begin{bmatrix} x_0 & \dot{x}_0 & \theta_0 & \dot{\theta}_0 \end{bmatrix}$ and reference signal r. For all simulation tests, simulation time and step size are chosen as $T = 5\,sec$ and $h = 0.001$, respectively.

In the first simulation test, for reference signal $r = 0$ and initial conditions $\begin{bmatrix} x_0 & \dot{x}_0 & \theta_0 & \dot{\theta}_0 \end{bmatrix} = \begin{bmatrix} 0 & 0 & 0.1 & 0 \end{bmatrix}$, the cart position (x), pendulum angle (θ) and control signal (u) are plotted and shown in Figure 7.2, Figure 7.3, and Figure 7.4, respectively.

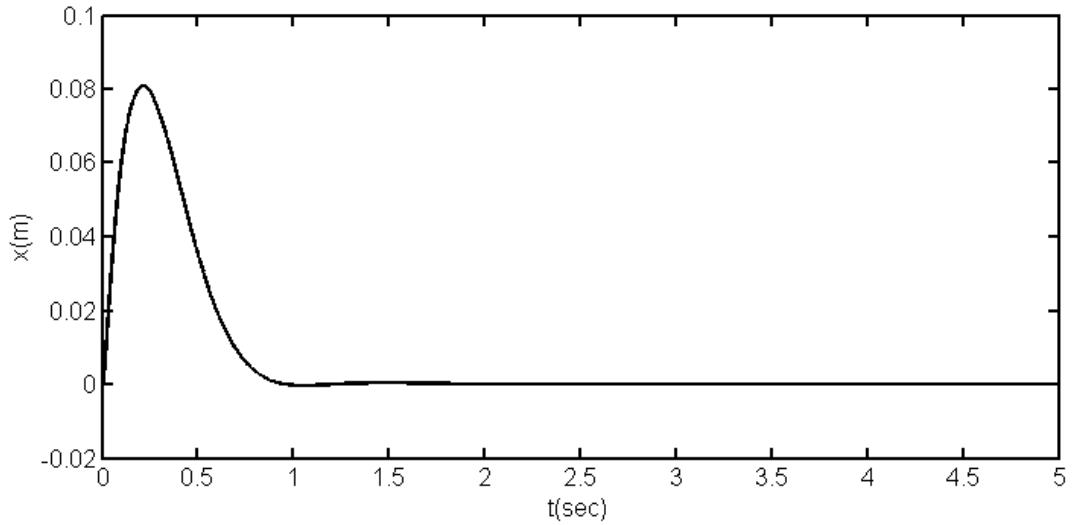

Figure 7.2. Cart position for $r = 0$ and initial conditions

$$\begin{bmatrix} x_0 & \dot{x}_0 & \theta_0 & \dot{\theta}_0 \end{bmatrix} = \begin{bmatrix} 0 & 0 & 0.1 & 0 \end{bmatrix}$$

The controller managed to keep the cart position in initial position while bringing the pendulum angle from $0.1\,rad$ to $0\,rad$ as shown in Figure 7.2. The cart moved to $0.08\,m$ from the initial position in $0.5\,sec$ and then return to the initial position in $1\,sec$.

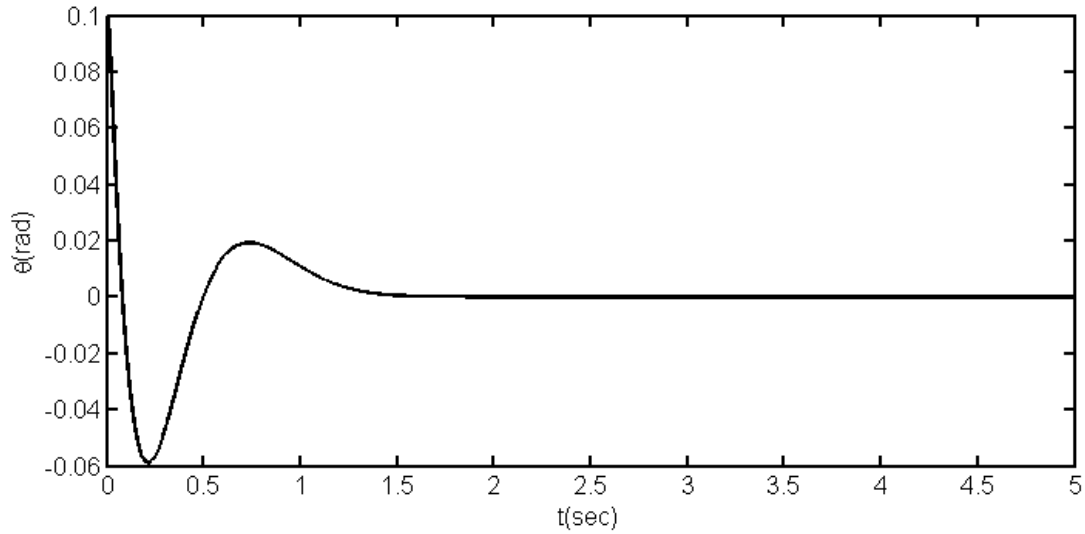

Figure 7.3. Pendulum angle for $r = 0$ and initial conditions

$$\begin{bmatrix} x_0 & \dot{x}_0 & \theta_0 & \dot{\theta}_0 \end{bmatrix} = \begin{bmatrix} 0 & 0 & 0.1 & 0 \end{bmatrix}$$

Since the main purpose of this study is to keep the pendulum in the upright position, the controller managed to bring the pendulum to upright position in about 1.5 *sec* as shown in Figure 7.3.

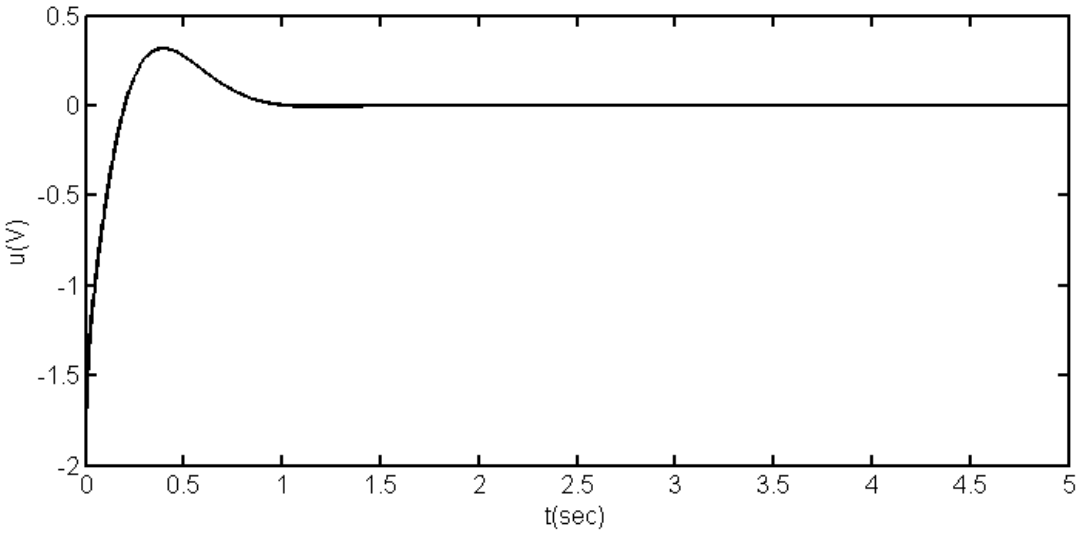

Figure 7.4. Control signal for $r = 0$ and initial conditions $\begin{bmatrix} x_0 & \dot{x}_0 & \theta_0 & \dot{\theta}_0 \end{bmatrix} = \begin{bmatrix} 0 & 0 & 0.1 & 0 \end{bmatrix}$

The control signal u started from $-1.5\,V$ and came to $0\,V$ in about $1.5\,sec$ in parallel to the pendulum angle. Also it is a smooth control signal, since it met the physical constraint which the control signal must be in the range of -2.5 V and +2.5 V.

In the second simulation test, for reference signal $r = 0.1$ and initial conditions $\begin{bmatrix} x_0 & \dot{x}_0 & \theta_0 & \dot{\theta}_0 \end{bmatrix} = \begin{bmatrix} 0 & 0 & 0 & 0 \end{bmatrix}$, the cart position (x), pendulum angle (θ) and control signal (u) are plotted and shown in Figure 7.5, Figure 7.6, and Figure 7.7, respectively.

In the second simulation test, the controller managed to keep pendulum in upright position ($\theta = 0\,rad$), while bringing the cart from the initial position $0\,m$ to desired position in about $1.5\,sec$ as shown in Figure 7.5. The pendulum angle came to $0.07\,rad$ from the initial position and then move to about $-0.03\,rad$ in about

0.6 *sec* after that it has reached to desired position 0 *rad* in about 1.5 *sec* as shown in Figure 7.6.

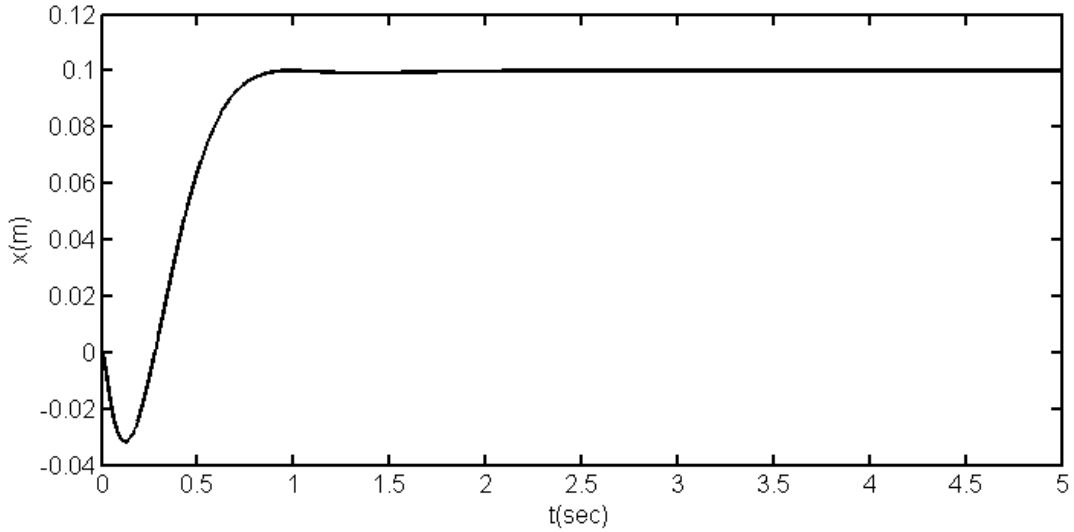

Figure 7.5. Cart position for $r = 0.1$ and initial conditions

$$\begin{bmatrix} x_0 & \dot{x}_0 & \theta_0 & \dot{\theta}_0 \end{bmatrix} = \begin{bmatrix} 0 & 0 & 0 & 0 \end{bmatrix}$$

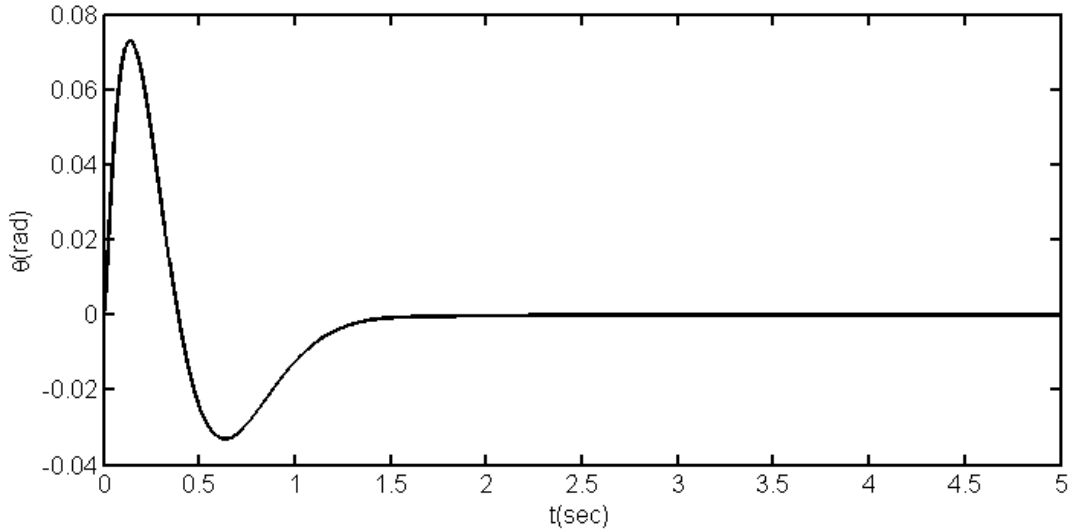

Figure 7.6. Pendulum angle for $r = 0.1$ and initial conditions

$$\begin{bmatrix} x_0 & \dot{x}_0 & \theta_0 & \dot{\theta}_0 \end{bmatrix} = \begin{bmatrix} 0 & 0 & 0 & 0 \end{bmatrix}$$

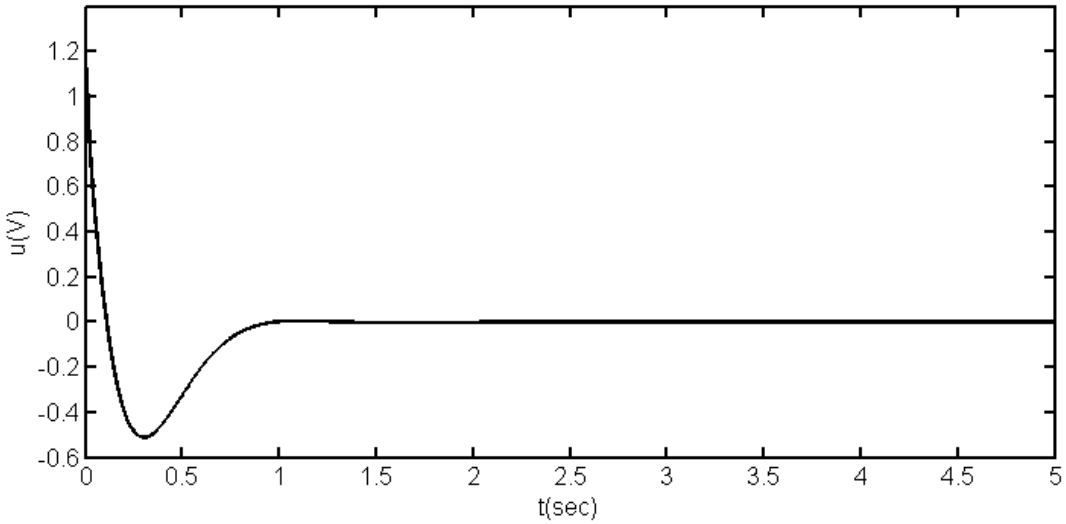

Figure 7.7. Control signal for $r = 0.1$ and initial conditions $\begin{bmatrix} x_0 & \dot{x}_0 & \theta_0 & \dot{\theta}_0 \end{bmatrix} = \begin{bmatrix} 0 & 0 & 0 & 0 \end{bmatrix}$

The control signal started from $1.2\,V$ and came to $-0.5\,V$ in about $0.4\,sec$ then it has reached $0\,V$ in about $1.5\,sec$. During the simulation it was in the range of -2.5 V and +2.5 V so it is a smooth control signal.

In the third simulation test, for reference signal $r = 0.1$ and initial conditions $\begin{bmatrix} x_0 & \dot{x}_0 & \theta_0 & \dot{\theta}_0 \end{bmatrix} = \begin{bmatrix} 0 & 0 & 0.1 & 0 \end{bmatrix}$, the cart position (x), pendulum angle (θ) and control signal (u) are plotted and shown in Figure 7.8, Figure 7.9, and Figure 7.10, respectively.

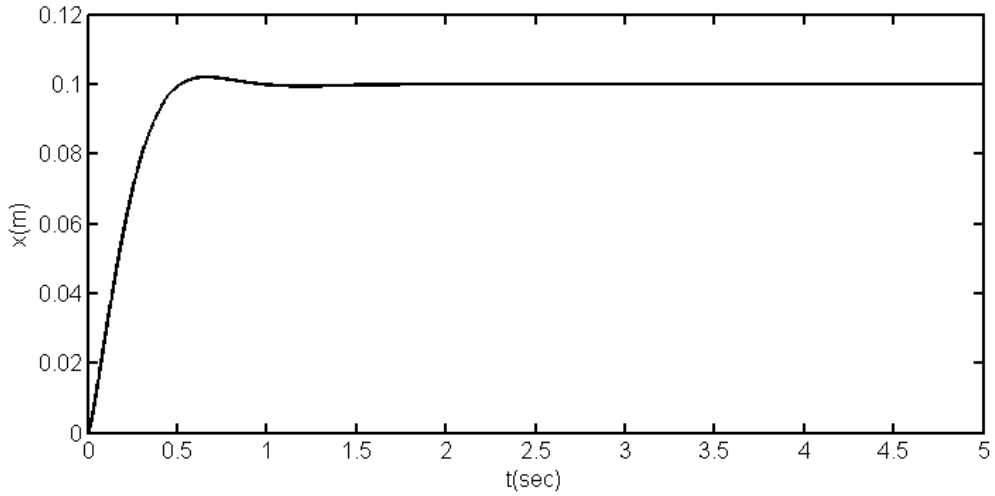

Figure 7.8. Cart position for $r = 0.1$ and initial conditions $\begin{bmatrix} x_0 & \dot{x}_0 & \theta_0 & \dot{\theta}_0 \end{bmatrix} = \begin{bmatrix} 0 & 0 & 0.1 & 0 \end{bmatrix}$

The controller managed to keep pendulum in upright position ($\theta = 0\,rad$), while bringing the cart from the initial position $0m$ to desired position in about $1\,sec$ as shown in Figure 7.8 in the third simulation test. The pendulum angle came to $-0.03\,rad$ from the initial position and then it reached to desired position $0\,rad$ in about $1\,sec$ as shown in Figure 7.9.

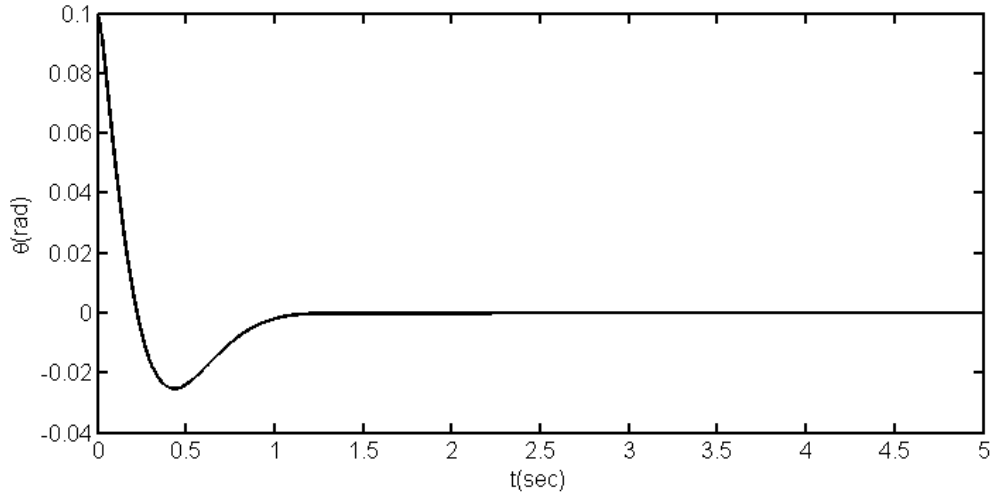

Figure 7.9. Pendulum angle for $r = 0.1$ and initial conditions $\begin{bmatrix} x_0 & \dot{x}_0 & \theta_0 & \dot{\theta}_0 \end{bmatrix} = \begin{bmatrix} 0 & 0 & 0.1 & 0 \end{bmatrix}$

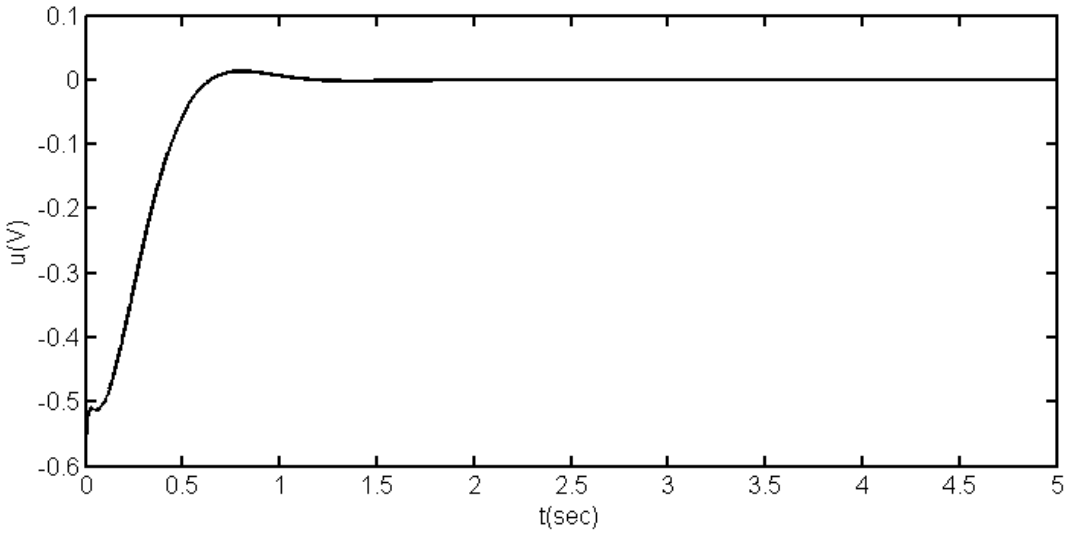

Figure 7.10. Control signal for $r = 0.1$ and initial conditions $\begin{bmatrix} x_0 & \dot{x}_0 & \theta_0 & \dot{\theta}_0 \end{bmatrix} = \begin{bmatrix} 0 & 0 & 0.1 & 0 \end{bmatrix}$

The control signal has started from about $-0.5\,V$ and has reached $0\,V$ in about $1\,sec$. During the simulation it was in the range of -2.5 V and +2.5 V so it is a smooth control signal.

In the fourth simulation test, for reference signal $r = 0.2$ and initial conditions $\begin{bmatrix} x_0 & \dot{x}_0 & \theta_0 & \dot{\theta}_0 \end{bmatrix} = \begin{bmatrix} 0 & 0 & 0 & 0 \end{bmatrix}$, the cart position (x), pendulum angle (θ) and control signal (u) are plotted and shown in Figure 7.11, Figure 7.12, and Figure 7.13, respectively.

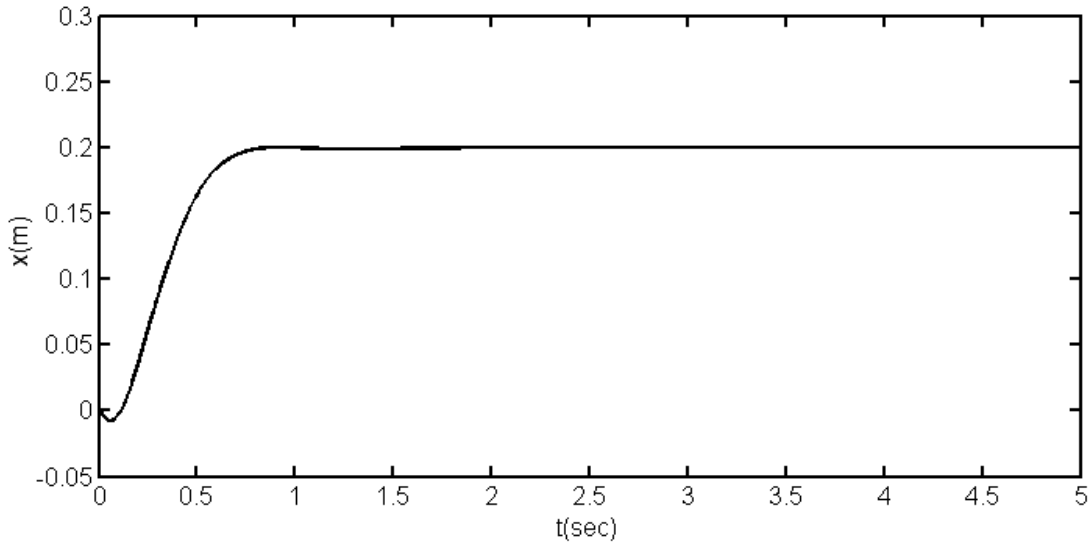

Figure 7.11. Cart position for $r = 0.2$ and initial conditions

$$\begin{bmatrix} x_0 & \dot{x}_0 & \theta_0 & \dot{\theta}_0 \end{bmatrix} = \begin{bmatrix} 0 & 0 & 0 & 0 \end{bmatrix}$$

The controller managed to keep pendulum in upright position ($\theta = 0\,rad$), while bringing the cart from the initial position $0\,m$ to desired position in about $0.7\,sec$ as shown in Figure 7.11 in the fourth simulation test. The pendulum angle came to $0.15\,rad$ from the initial position and then move to about $-0.07\,rad$ in about $0.6\,sec$ after that it has reached to desired position $0\,rad$ in about $1.5\,sec$ as shown in Figure 7.12.

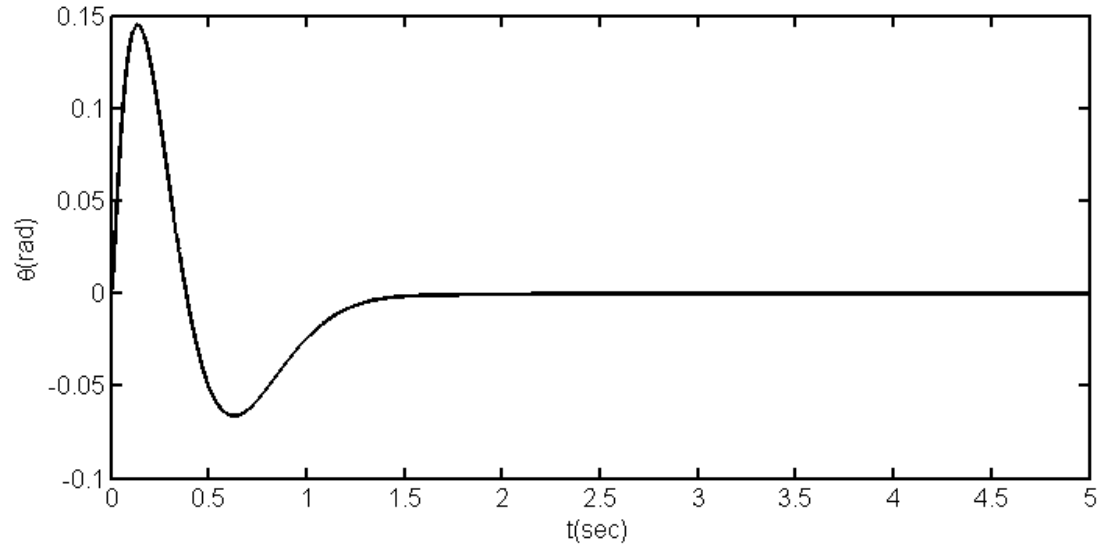

Figure 7.12. Pendulum angle for $r = 0.2$ and initial conditions $\begin{bmatrix} x_0 & \dot{x}_0 & \theta_0 & \dot{\theta}_0 \end{bmatrix} = \begin{bmatrix} 0 & 0 & 0 & 0 \end{bmatrix}$

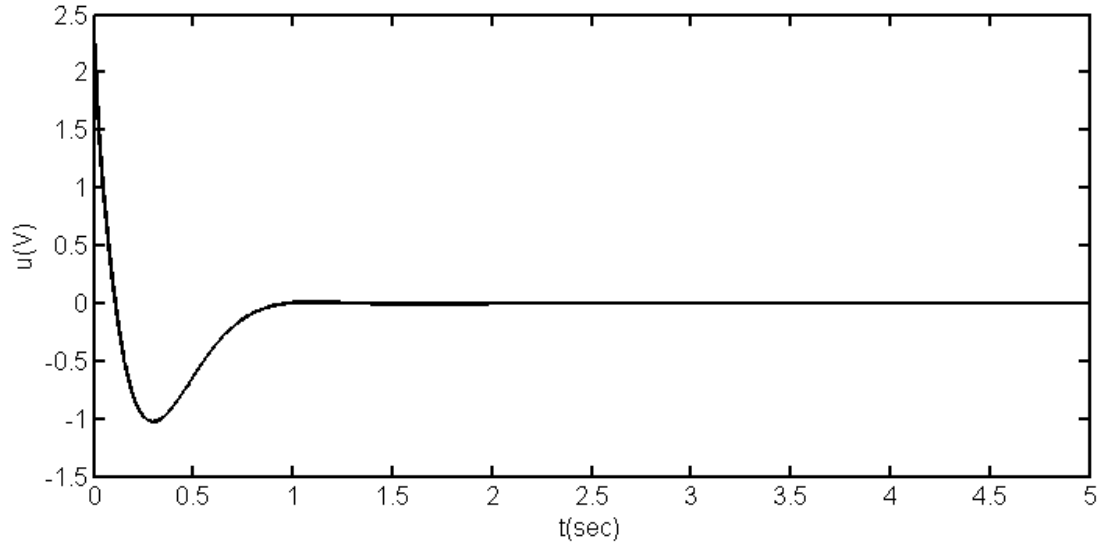

Figure 7.13. Control signal for $r = 0.2$ and initial conditions $\begin{bmatrix} x_0 & \dot{x}_0 & \theta_0 & \dot{\theta}_0 \end{bmatrix} = \begin{bmatrix} 0 & 0 & 0 & 0 \end{bmatrix}$

The control signal started from $2.3\,V$ and came to $-1\,V$ in about $0.4\,sec$ then it has reached $0\,V$ in about $1.5\,sec$. During the simulation it was in the range of -2.5 V and +2.5 V so it is a smooth control signal.

However during the simulations a satisfactory performance was obtained, comparing the proposed method with another method will provide a clearer view

about the performance. Some of the methods proposed in the literature are mentioned before. The method proposed by Ghosh et al. in 2012 is used for comparison purposes in this study. According to this method Q and R matrices can be defined as follows (Ghosh et al., 2012):

$$\left.\begin{aligned} Q &= diag\{q_{11}, q_{22}, q_{33}, q_{44}\} \\ R &= r_{11} \end{aligned}\right\} \tag{7.3}$$

where $q_{11} = 500q$, $q_{22} = q_{33} = 20q$, $q_{44} = q$ and $r = 10^n$. By trial and error that with the choices $q = 100$ and $n = 4$, Q and R matrices are obtained as follows:

$$Q = \begin{bmatrix} 50000 & 0 & 0 & 0 \\ 0 & 2000 & 0 & 0 \\ 0 & 0 & 2000 & 0 \\ 0 & 0 & 0 & 100 \end{bmatrix}$$

$$R = [10000]$$

To obtain feedback gain matrix for this method the algebraic Ricatti equation given in Equation (4.21) is solved for P

$$A^T P + PA - PBR^{-1}B^T P + Q = 0$$

where A and B given in Equation (6.7) , Q and R given above. Then using the Equation (4.19)

$$K = R^{-1}B^T P$$

the feedback gain matrix for comparison is obtained as

$$K_c = \begin{bmatrix} 2.2361 & 4.2263 & 9.8447 & 2.0998 \end{bmatrix}$$

Based on K_c and matrices A , B and C which are given in Equation (6.7) and Equation (6.8), scale factor can be determined as

$$\bar{N}_c = 2.2361$$

The proposed method and the method proposed by Ghosh et al.(2012) are simulated in the simulation setup which is shown in Figure 7.1. The differences between these simulations are the feedback gain matrix K and the scale factor $\bar{N}$. For the proposed method the feedback matrix $K = \begin{bmatrix} 12.3579 & 8.1225 & 18.0051 & 4.0557 \end{bmatrix}$ and pre-compensation scale factor $\bar{N} = 12.3579$ are defined in Equation (7.1) and Equation (7.2), respectively, and also for the method proposed by Ghosh et al. (2012) the feedback matrix and pre-compensation scale factor are defined as $K_c = \begin{bmatrix} 2.2361 & 4.2263 & 9.8447 & 2.0998 \end{bmatrix}$ and $\bar{N}_c = 2.2361$, respectively. For both methods performance results are presented in Table 7.1 where initial conditions $x = 0$, $\theta = 0$ and reference signal $r = 0.2$. Also simulation time and step size are defined as $T = 10\ sec$ and $h = 0.001$. Cart position, pendulum angle and control signal are plotted in Figure 7.13, 7.14 and 7.15, respectively.

Table 7.1. Performance Results

	Method Proposed by Ghosh et al. (2012)	**Proposed Method**
t_s(sec)	2.6610	0.7340
$os(\%)$	2.1573×10^{-4}	3.0416×10^{-4}
e_{ss}	9.2345×10^{-6}	5.4496×10^{-8}
f_{sum}	2.6612	0.734003

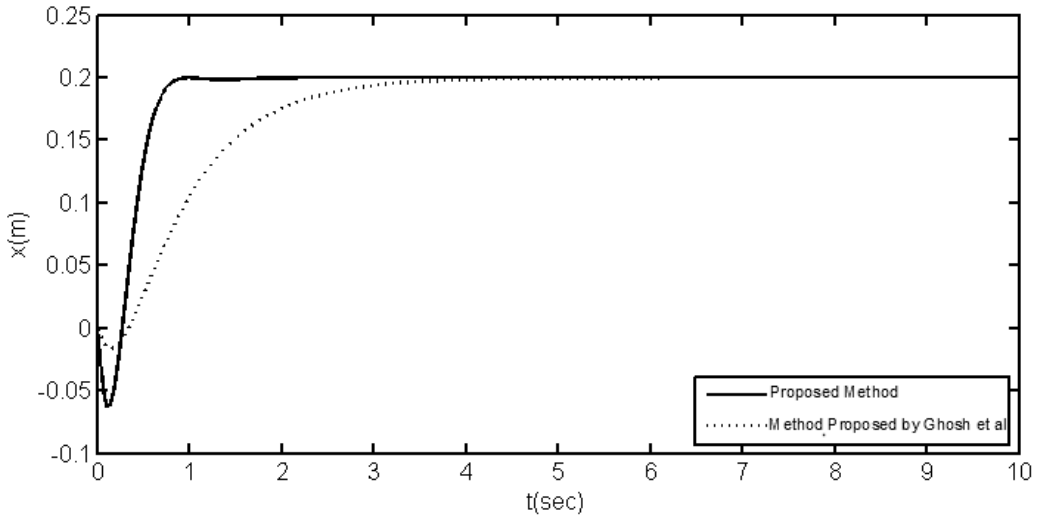

Figure 7.14. Comparison results of cart positions for $r = 0.2$ and initial conditions $\begin{bmatrix} x_0 & \dot{x}_0 & \theta_0 & \dot{\theta}_0 \end{bmatrix} = \begin{bmatrix} 0 & 0 & 0 & 0 \end{bmatrix}$

The proposed method was indicated by solid line and the other method was indicated by dotted line in these figures. The proposed method is faster about three times than the other method as shown in Figure 7.14. The cart reached the desired position (0.2 m) in about 0.75 *sec* with the proposed method while it took 2.7 *sec* in the other method.

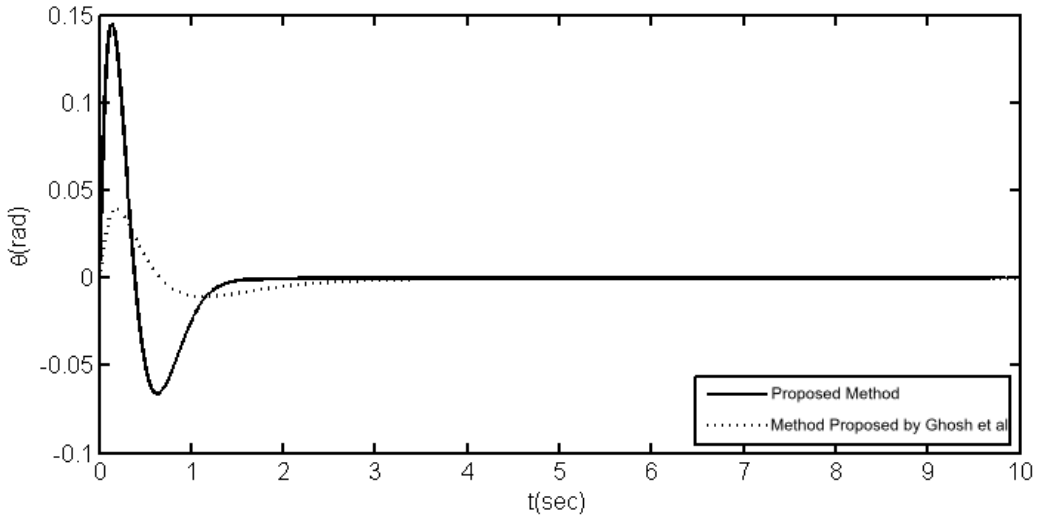

Figure 7.15. Comparison results of pendulum angles for $r = 0.2$ and initial conditions $\begin{bmatrix} x_0 & \dot{x}_0 & \theta_0 & \dot{\theta}_0 \end{bmatrix} = \begin{bmatrix} 0 & 0 & 0 & 0 \end{bmatrix}$

Pendulum's swinging bound for the proposed method is a bit larger than the other method as shown in Figure 7.15, despite the proposed method managed to keep the pendulum upright position in about $1\,sec$ while it took about $2\,sec$ for the other method.

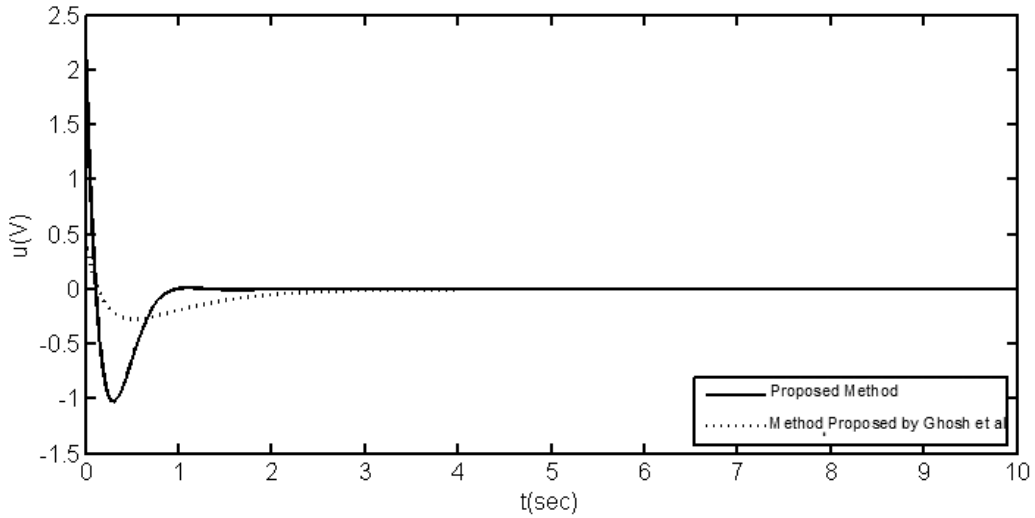

Figure 7.16. Comparison results of control signals for $r = 0.2$ and initial conditions $\begin{bmatrix} x_0 & \dot{x}_0 & \theta_0 & \dot{\theta}_0 \end{bmatrix} = \begin{bmatrix} 0 & 0 & 0 & 0 \end{bmatrix}$

Although the control signal produced by the proposed method was higher than the other method, it was still a smooth control signal in $\begin{bmatrix} -2.5V & +2.5V \end{bmatrix}$ bound.

Overall, the simulation results have shown that the proposed method is more efficient than the method proposed by Ghosh et al. (2012) to select weighting matrices for LQR controller design.

8. CONCLUSION AND FUTURE WORK

The current study has presented a new ABC algorithm based strategy that focuses on efficiency of LQR controller design process. The ABC algorithm has been employed to determine LQR controller weighting matrices and an LQR controller has been designed for an inverted pendulum system with DC motor. The designed LQR controller was tested with different reference signals and different initial conditions. It is well known that the ABC algorithm has good performances in solving numerical optimization problems. Thus, the effectiveness of the LQR controller design using the ABC algorithm was researched and a satisfactory performance was obtained.

The simulation results have shown that using the ABC algorithm is more effective and feasible to select weighting matrices for LQR controller design than the method proposed by Ghosh et al. (2012). Also it has shown that the proposed method can optimize multiple time domain control system specifications such as settling time, overshot and steady state error, simultaneously.

The proposed method is flexible and applicable in a wide range of optimization problems. Hence, it can be regarded as a general controller design method that can be applied to a wide class of control problems.

Although, the simulation test outcomes for the proposed method have effective results, it could be compared with other swarm intelligence algorithms such as PSO and GA.

There may exist some varying parameters, disturbances, and uncertainties in the real-life plants. Moreover, an exact mathematical model cannot be obtained. For this reason, this proposed control system which has exhibited a very good performance in simulation might not give satisfying results in real life implementations. Since this thesis is mainly intended to provide a sufficient algorithm based on the ABC algorithm for optimizing the weighting matrices Q and R of LQR controller in accordance with some time-domain performance criteria, a simple LQR control configuration has been adopted and tested in simulation. Practical control design in real-life applications remains for an interesting future

work. In such a design addition of an integral control part in LQR may be required. Furthermore, some improvements for the mathematical model of the plant in hand may be needed to get a more realistic model. These improvements can include: (1) not to neglect inductance L and viscous damping D of the DC motor, (2) to add a new state variable for force F in the state space model of the inverted pendulum with DC motor.

The proposed method would be useful for more complex plants. Testing the method for such plants would be interesting for future work.

REFERENCES

AKAY, B., and KARABOGA, D., 2009a. Solving integer programming problems by using artificial bee colony algorithm. In: Emergent Perspectives in Artificial Intelligence. Springer Berlin Heidelberg. p. 355-364.

AKAY, B., and KARABOGA, D., 2009b. Parameter tuning for the artificial bee colony algorithm. In Computational collective intelligence. Semantic web, social networks and multiagent systems. Springer Berlin Heidelberg. p. 608-619.

BASTURK, B., KARABOGA, D., 2006. An artificial bee colony (ABC) algorithm for numeric function optimization. In: IEEE swarm intelligence symposium, p: 12-14.

ANDERSON, C. W., 1989. Learning to control an inverted pendulum using neural networks. Control Systems Magazine, IEEE, 9(3):31-37.

ÅSTRÖM, K. J., and FURUTA, K., 2000. Swinging up a pendulum by energy control. Automatica, 36(2):287-295.

ATHANS, M., 1966. The status of optimal control theory and applications for deterministic systems. Automatic Control, IEEE Transactions on, 11(3):580-596.

AYRES Jr, F.,1962. Matrices, Schaum's Outline Series.Schaum Publishing, New York, 230p.

BONABEAU, E., DORIGO, M., and THERAULAZ, G., 1999. Swarm intelligence: from natural to artificial systems, Oxford University Press, 307p.

BONABEAU, E., MEYER, C., 2001. Swarm intelligence: A whole new way to think about business. Harvard Business Review, 79(5):106-115.

BOTTURA, C. P., DA FONSECA NETO, J. V., 2000. Rule-based decision-making unit for eigenstructure assignment via parallel genetic algorithm and LQR designs. In Proceedings of the American Control Conference, 1(6):467-471.

BRYSON, A. E., HO, Y. C., 1975. Applied Optimal Control: Optimization, Estimation, and Control. Taylor & Francis Group, 496p.

COBAN, R., 2011. A fuzzy controller design for nuclear research reactors using the particle swarm optimization algorithm. Nuclear Engineering and Design, 241(5): 1899-1908.

DA FONSECA NETO, J. V., ABREU, I. S., and DA SILVA, F. N., 2010. Neural–Genetic Synthesis for State-Space Controllers Based on Linear Quadratic Regulator Design for Eigenstructure Assignment. Systems, Man, and Cybernetics, Part B: Cybernetics, IEEE Transactions 40(2): 266-285.

ERCIN, O., COBAN, R., 2012. Identification of linear dynamic systems using artificial bee colony algorithm. Turkish Journal of Electrical Engineering & Computer Sciences, 20(1):1175-1188.

FEEDBACK INSTRUMENTS LTD., 2006. 33-936S Digital pendulum control experiments manual.

FRANKLIN, G. F., WORKMAN, M. L., and POWEL, D., 2006. Digital control of dynamic systems. Ellis-Kagle Press, 732p.

GHOSH, A., KRISHNAN, T. R., and SUBUDHI, B., 2012. Robust proportional–integral–derivative compensation of an inverted cart–pendulum system: an experimental study. IET control theory & applications, 6(8): 1145-1152.

IFAC THEORY COMMITTEE, 1990, Benchmark Problems.

JEONG, S., TAKAHASHI, T., 2007. Wheeled inverted pendulum type assistant robot: inverted mobile, standing, and sitting motions. Intelligent Robots and Systems, IEEE/RSJ International Conference on, p: 1932-1937.

KALMAN, R. E., 1964. When is a linear control system optimal? Journal of Fluids Engineering, 86(1): 51-60.

KARABOGA, D., 2005. An idea based on honey bee swarm for numerical optimization. Technical Report TR06, Erciyes University Press, Kayseri.

KARABOGA, D. AKAY, B., 2009. A comparative study of artificial bee colony algorithm. Applied Mathematics and Computation, 214(1):108-132.

KARABOGA, D., BASTURK, B., 2007. A powerful and efficient algorithm for numerical function optimization: artificial bee colony (ABC) algorithm. Journal of global optimization, 39(3): 459-471.

KARABOGA, D., BASTURK, B., 2008. On the performance of artificial bee colony (ABC) algorithm. Applied soft computing, 8(1): 687-697.

KIRK, D. E., 2012. Optimal control theory: an introduction. Courier Dover Publications, 464p. (Reprint of the Prentice-Hall, Inc., Englewood Cliffs, New Jersey, 1970 edition)

KUO, A. D., 2007. The six determinants of gait and the inverted pendulum analogy: A dynamic walking perspective. Human movement science, 26(4): 617-656.

KWAKERNAAK, H., SIVAN, R., 1972. Linear optimal control systems. Wiley, New York, 608p.

MABLEKOS, V. E., 1980, Electric Machine Theory For Power Engineers. Harper and Row, New York, 698p.

MESSNER, W., and TILBURY, D., 2011. Inverted Pendulum: State-Space Methods for Controller Design in Control Tutorials for Matlab and Simulink. Online available:http://ctms.engin.umich.edu/CTMS/index.php?example=InvertedPendulum&section=ControlStateSpace

MOBAYEN, S., RABIEI, A., MORADI, M., and MOHAMMEDY, B., 2011. Linear quadratic optimal control system design using particle swarm optimization algorithm. International Journal of the Physical Sciences, 6(30): 6958-6966.

NAKRANI, S., TOVEY, C., 2004. On Honey Bees and Dynamic Allocation in Internet Hosting Centers. Adaptive Behavior, 12(3-4):223-240.

NISE, N.S., 2004. Control System Engineering (4th Edition). Wiley, 983p.

OGATA, K., 1995. Discrete-time control systems (2nd Edition). Prentice Hall, 745p.

TEODOROVIC, D., DELL'ORCO, M., 2005. Bee colony optimization – A cooperative learning approach to complex transportation problems. In Advanced OR and AI Methods in Transportation. Proceedings of the 10th Meeting of the EURO Working Group on Transportation, Poznan, Poland, 51–60.

TERESHKO, V., 2000. Reaction-diffusion model of a honeybee colony's foraging behaviour. Parallel Problem Solving from Nature PPSN VI, Springer, Berlin, 807-816.

YAOQING, W., 1992. The determination of weighting matrices in LQ optimal control system. Acta Automatica Sinica, 2: 011.

CURRICULUM VITAE

Barış ATA was born in Akşehir, in 1986. He completed university education at department of Computer Engineering of Kocaeli University in 2010. Since 2012, he has been working as a research assistant at Computer Engineering Department of Çukurova University in Adana.